Therapy with ^{177}Lu- octreotate

Pharmacokinetics, dosimetry and kidney toxicity

Maria Larsson

Department of Radiation Physics
Institute of Clinical Sciences
Sahlgrenska Cancer Center
Sahlgrenska Academy at University of Gothenburg

UNIVERSITY OF GOTHENBURG

Gothenburg 2014

Therapy with ^{177}Lu-octreotate

maria.larsson@radfys.gu.se

ISBN 978-91-628-8916-6
E-publication: http://hdl.handle.net/2077/35451

Printed in Gothenburg, Sweden 2014
Aidla Trading AB/Kompendiet, Gothenburg

To my family with love

I think I did it!

”My Mama always said you've got to put the past behind you before you can move on.”

Forrest Gump

SAMMANFATTNING PÅ SVENSKA

^{177}Lu-octreotate används för behandling av patienter med neuroendokrina tumörer som uttrycker somatostatin-receptorer vid vissa kliniker. I allmänhet används liknande behandlingsschema Sammanfattningsvis är njur- och benmärgstoxicitet det som begränsar behandling med ^{177}Lu-octreotate. Resultaten är lovande, men behandlingsschemat har inte optimerats och djurstudier visar att fler patienter borde kunna botas. För att optimera behandling och minimera toxiciteten behövs mer kunskap om individuell biodistribution och dosimetriska data. De biologiska effekterna på njurvävnad från bestrålning med ^{177}Lu måste studeras, liksom bättre sätt att blockera retentionen av radionuklid i njurarna.

De specifika målen för projektet var att bestämma farmakokinetiken i patienter, samt att utföra dosimetriska uppskattningar för njure, benmärg, lever, mjälte och tumörer efter administrering av ^{177}Lu-octreotate, att studerade radiobiologiska effekterna av ^{177}Lu på njurarna i en djurmodell, och att studera hur lysin och dimercaptosuccinic acid (DMSA) påverkar upptaget av ^{111}In-octreotide i njurarna.

Farmakokinetiken i patienter som erhållit 3,5-8 GBq ^{177}Lu-octreotate upp till sex gånger kombinerat med aminosyror för att blockera upptaget i njurarna bestämdes från planara scintigrafiska bilder och conjugate-view-metoden. Stora individuella variationer observerades för absorberade dos per administrerad aktivitet för alla vävnader, t ex 0,33–2,4 Gy/GBq till njurarna, 0,047-0,54 Gy/GBq till levern, 0.28-4.4 Gy/GBq till mjälten, och 0,010-0,093 Gy/GBq till benmärg. Tumörvävnaden erhöll upp till 20 Gy/GBq.

Långtidseffekter på njurarna studerades efter injektion med 0-150 MBq ^{177}Lu-octreotate i normala möss. Effekter på njurfunktioner, så som glomulär filtrering, reabsorption och exkretion observerades efter injektion med hög aktivitet med hjälp av ^{99m}Tc-DTPA--scintigrafi och ureanivåer i blod. Resultaten kan vara viktiga för att definiera potentiella biomarkörer för tidig prediktion av sen njurtoxicitet.

Blockering av upptaget av ^{111}In-octreotide i njurarna studerades in normala möss med hjälp av lysin och DMSA. Resultaten visade att upptaget av ^{111}In beror på den administrerade mängden lysin och DMSA, samt tid för injektion av dessa substanser. Lysin kombinerat med DMSA gav ej bättre blockering, troligtvis på mindre lämpliga tider för injektion.

Sammanfattningsvis visar detta arbete att det är viktigt och möjligt att optimera behandling av patienter med neuroendokrina tumörer med ^{177}Lu-octreotate.

Therapy with ^{177}Lu- octreotate

Pharmacokinetics, dosimetry and kidney toxicity

Maria Larsson

Department of Radiation Physics, Institute of Clinical Sciences
Sahlgrenska Cancer Center
Sahlgrenska Academy at University of Gothenburg
Göteborg, Sweden

ABSTRACT

^{177}Lu-octreotate is used for treatment of patients with somatostatin receptor expressing neuroendocrine tumors in some clinics using a standard schedule. Renal and bone marrow toxicity are the main limiting factors. Results are in general positive, but no optimization of treatment schedule has been performed and animal studies suggest that higher cure rate might be possible. To optimize the treatment and minimize toxicity, individual biodistribution and dosimetric data are needed. The biological effects on kidney tissue of ^{177}Lu must be studied, together with better ways to block the radionuclide retention in kidneys.

The aims of the project were to determine the pharmacokinetics in patients and to perform dosimetric estimations for kidneys, bone marrow, liver, spleen and tumors after ^{177}Lu-octreotate administration, to examine the radiobiological effects of ^{177}Lu in the kidneys in an animal model, and to study how kidney blocking agents lysine and dimercaptosuccinic acid (DMSA) affect the uptake of ^{111}In-octreotide in the kidneys.

The pharmacokinetics in patients who received 3.5-8 GBq ^{177}Lu-octreotate up to six times combined with amino acids for kidney blocking, were determined using planar scintigraphy and conjugate view method. Large individual variations were observed in absorbed dose per administered activity to all tissues, e.g. 0.33-2.4 Gy/GBq to kidneys, 0.047-0.54 Gy/GBq to liver, 0.28-4.4 Gy/GBq to spleen, and 0.010-0.093 Gy/GBq to bone marrow. Tumors received up to 20 Gy/GBq.

Long-term effects on the kidneys after injection of 0-150 MBq ^{177}Lu–octreotate were evaluated in normal mice. Effects on renal functions, e.g. glomerular filtration, reabsorption, and excretion were observed after high administered activity using ^{99m}Tc-DTPA–scintigraphy and urea level in blood. Results may be important for defining potential biomarkers for early prediction of late renal toxicity and impairment.

Blocking of the uptake of ^{111}In-octreotide in the kidneys was studied in normal mice using lysine and DMSA. The results indicated that the uptake of ^{111}In depends on the amount of lysine and DMSA administered, and the time for injection of respective agent. Lysine combined with DMSA did not give better blocking, probably due to less optimal time schedule.

In conclusion, this work demonstrates the importance and some possibilities to optimize treatment of patients with neuroendocrine tumors using ^{177}Lu-octreotate.

Keywords: PRRT, ^{177}Lu-octreotate, ^{111}In-octreotide, dosimetry, biokinetics, scintigraphy, conjugate view method, renal function, renal toxicity, lysine, DMSA, ^{99m}Tc-DTPA, ^{99m}Tc-DMSA

ISBN: 978-91-628-8916-6

E-publication: http://hdl.handle.net/2077/35451

LIST OF PAPERS

This thesis is based on the following studies, referred to in the text by their Roman numerals.

I. Maria Larsson, Peter Bernhardt, Johanna B Svensson, Bo Wängberg, Håkan Ahlman, Eva Forssell-Aronsson. Estimation of absorbed dose to the kidneys after treatment with ^{177}Lu-octreotate: comparison between methods based on planar scintigraphy. EJNMMI Research 2012, 2:49.

II. Maria Larsson, Peter Bernhardt, Johanna B Svensson, Bo Wängberg, Eva Forssell-Aronsson. Mean absorbed doses estimation to liver, spleen and tumors tissue in patients with neuroendocrine tumors after treatment with ^{177}Lu-octreotate. Manuscript.

III. Emil Schüler, Maria Larsson, Toshima Z. Parris, Martin Johansson, Khalil Helou, Eva Forssell-Aronsson. Biomarkers for radiation-induced renal toxicity following ^{177}Lu-octreotate administration in mice. Manuscript.

IV. Maria Larsson, Andreas Österlund, Emil Schüler, Eva Forssell-Aronsson. Evaluation of DMSA and lysine as kidney protecting agents in C57BL/6N mice. Submitted

OTHER RELATED PUBLICATIONS AND PRESENTATIONS

Publications

Swärd C, Bernhardt P, Ahlman H, Wängberg B, Forssell-Aronsson E, Larsson M, Svensson J, Rossi-Norrlund R, Kölby L. [^{177}Lu-DOTA^{0}-Tyr^{3}]-octreotate treatment in patients with disseminated gastroenteropancreatic neuroendocrine tumors: the value of measuring absorbed dose to the kidney. World J Surg 2010; 34:1368–1372

Presentations

Larsson M. Dosimetric estimation of kidney dose after patient treatments with ^{177}Lu-DOTA^{0},Tyr^{3}-octreotate on neuroendocrine somatostatin-receptor-expressing tumour. Quantitative imaging and dosimetry symposium. Berder Island, France, 2008

Larsson M, Bernhardt P, Ahlman H, Wängberg B, Forssell-Aronsson E. Dosimetric estimation of kidney dose after patient treatments with ^{177}Lu-DOTA^{0},-Tyr^{3}-octreotate on neuroendocrine somatostatin-receptor-expressing tumour. Cancerfondens planeringsgrupp för onkologisk nuklidterapi och Svensk Förening för Isotopterapi Linköping 2008

Larsson M, Bernhardt P, Berg G, Svensson J, Ahlman H, Wangberg B, Forssell-Aronsson E. Estimation of absorbed dose to the kidneys after treatment with ^{177}Lu-DOTA-octreotate. SNM Annual Meeting, Toronto, June 13-17, 2009

Sward C, Bernhardt P, Forssell-Aronsson E, Berg G, Svensson J, Larsson M, Norrlund R, Kolby L. [^{177}Lu-DOTA^{0}-Tyr^{3}]-octreotate treatment in patients with gastroenteropancreatic neuroendocrine tumours - the value of measuring absorbed dose to the kidneys. International Surgical Week, Adelaide, Australia, September 7-10, 2009

Larsson M, Bernhardt P, Ahlman H, Wängberg B, Forssell-Aronsson E. Absorberad dos till njure hos patienter som behandlats med ^{177}Lu-[DOTA^{0},Tyr^{3}] octreotate. Cancerfondens planeringsgrupp för onkologisk nuklidterapi samt Svensk förening för isotopterapi Lund 2010

Larsson M, Bernhardt P, Ahlman H, Wängberg B, Forssell-Aronsson E. Absorbed dose to the kidneys after treatment with ^{177}Lu-octreotate. Annual Congress of European Association of Nuclear Medicine, Birmingham, 2011

Larsson M, Bernhardt P, Svensson J, Ahlman H, Wangberg B, Forssell-Aronsson E. Absorbed dose to the kidneys after treatment with ^{177}Lu-octreotate. Swedish Radiation Research Association for Young Scientists (Swe-Rays) workshop, Stockholm 2012 (Oral presentation)

Larsson M, Schüler E, Parris T, Rudqvist N, Helou K, Ahlman H, Forssell-Aronsson E. Kidney toxicity in mice treated with [^{177}Lu-DOTA^{0}-Tyr^{3}]-octreotate. Annual Congress of European Association of Nuclear Medicine, Milano, 2012

Svensson J, Hermann R, Larsson M, Forssell-Aronsson E, Wängberg B, Ahlman H, Bernhardt P. Impairment in renal function predicts higher absorbed doses to the kidneys in peptide receptor radionuclide therapy. Annual Congress of European Association of Nuclear Medicine, Milano, 2012

Magnander T, Engström A, Svensson J, Larsson M, Forssell-Aronsson E, Ahlman H, Wängberg B, Bernhardt P. SPECT based method for determining the reliability of background ROIs used in conjugate view technique. Annual Congress of European Association of Nuclear Medicine, Milano, 2012

Invited speaker

Larsson M, Bernhardt P, Ahlman H, Wängberg B, Forssell-Aronsson E. Absorberad dos till njure hos patienter som behandlats med ^{177}Lu-[DOTA^{0},Tyr^{3}] octreotate. Radiofysikdagen 2010, anordnad av Svensk Förening för Radiofysik i anslutning till Läkaresällskapets riksstämma, 2010

CONTENT

ABBREVIATIONS

AJCC	American Joint Committee on Cancer
BM	Bone metastases
CHO-K1	Chinese hamster ovary cells line
CV	Conjugate view
DMSA	Dimercaptosuccinic acid
DOTA	1,4,7,10-tetraaza-cyclododecane-1,4,7,10-tetraacetic acid
DTPA	Diethylene triamine pentaacetic acid
EANM	European Association of Nuclear Medicine
EDTA	Ethylenediamine tetraacetic acid
ENETS	European Neuroendocrine Tumor Society
ER	Endoplasmic reticulum
FDA	The U.S. food and drug administration
GFR	Glomerular filtration rate
GRK	G-protein-coupled receptor-kinase
Gy	Gray, SI unit for absorbed dose (1 Gy = 1 J/kg)
kDa	Kilo dalton, unified atomic mass unit (1 Da = 1 mol/g)
LM	Liver metastases
MIRD	Medical Internal Radiation Dose
NANETS	North American Neuroendocrine Tumor Society
NE	Neuroendocrine
NET	Neuroendocrine tumor
OM	Other metastases
PET	Positron emission tomography
PRRT	Peptide receptor radionuclide therapy
RIT	Radioimmunotherapy
ROI	Region-of-interest
SPECT	Single-photon emission computed tomography
SST	Somatostatin
SSTR	Somatostatin receptor
WHO	World Health Organization

1 INTRODUCTION

Therapy of neuroendocrine tumors with the radiolabeled somatostatin analogue ^{177}Lu[DOTA^{0},Tyr^{3}]octreotate (^{177}Lu-octreotate) show promising results, with prolonged tumor response and increased quality of life (Kwekkeboom, et al., 2010). However, few patients obtain complete remission, and ^{177}Lu-octreotate administration is often restricted to spare the limiting organs, i.e., kidneys and bone marrow. There is a need for enhanced knowledge about biodistribution, dosimetry and toxicity for better optimization of this treatment modality (Forssell-Aronsson, et al., 2013). The papers included in this thesis deal with various aspects of treatment of patients with neuroendocrine tumors using ^{177}Lu-octreotate. Radiolabeled peptides such as ^{177}Lu-octreotate are mainly cleared via the kidneys and to some extent reabsorbed and retained in the kidneys. Thus, one of the main limitations of therapy using radiolabeled peptides is renal toxicity. The main foci for the papers are pharmacokinetics, biodistribution, and dosimetry (Paper I and II), renal toxicity (Paper III), and the effect of blocking agents on kidney uptake (Paper IV).

1.1 Neuroendocrine tumors

Neuroendocrine tumors (NET) develop from neuroendocrine (NE) cells or their progenitor cells. The normal NE cells are present in the endocrine glands, e.g. pituitary gland, pancreas, gastrointestinal tract and adrenal gland. Overall the NE cells receive signals from the nervous system, to release hormones that trigger action in other endocrine glands or tissues.

NET can develop in many organs, most common in the gastrointestinal tract or the broncho-pulmonary system, and to a smaller extend in pancreas, testes, ovaries and the hepatobilary system (Gustafsson, et al., 2008). The primary tumors are often small and slow-growing, and it is therefore not uncommon that patients at time of diagnosis already have a metastatic disease.

Traditionally, gastrointestinal NETs were classified according to the location of the primary tumor: foregut (lung, thymus, stomach, pancreas and proximal duodenum), midgut (distal duodenum to the proximal transverse colon), and hindgut (distal colon and rectum) carcinoids. Later, the World Health Organization (WHO), the European Neuroendocrine Tumor Society (ENETS), the American Joint Committee on Cancer (AJCC), and the North American Neuroendocrine Tumor Society (NANETS) have been dealing

with nomenclature to classify the pathological staging and grading of the NETs. Guidelines have been set up, and the American system classifies the tumors in two families: well differentiated and poorly differentiated, while the European system classifies the tumors depending on the protein antigen KI 67 (Ki-67) proliferation index, using low, intermediate and high grade classification (Filice, et al., 2012, Klimstra, 2013).

Gennerally, a highly differentiated NE tumor cell has a low to intermediate proliferation rate, while a less differentiated cell has a high proliferating rate. The highly proliferating NET cells are more aggressive (e.g. grow faster and more invasively) (Klimstra, et al., 2010). For a complete pathological classification the tumor size, knowledge of invasion and location of metastases and presence of tumor markers are used. Treatment is based on tumor status, differentiation grade, origin, functional activity and receptor expression. Many NETs overexpress various hormone receptors on the tumor cell surface (Bodei, et al., 2009, Reubi, et al., 1987). One of the important receptors is somatostatin (SST) receptors (SSTR).

Patients with NET are generally treated with conventional multimodal therapy, e.g. surgery, chemotherapy, SST analogs, liver embolization and sometimes liver transplantation (Sward, et al., 2010). Today, targeted radionuclide therapy using radiolabeled SST analogues is usually initiated in a late stage of the disease progression, often when the patient is in a bad physical condition.

1.2 Somatostatin

Somatostatin (SST) (also known as somatotropin release inhibiting factor, SRIF) was identified in the 1970s and was initially revealed as an inhibitor of the secretion of growth hormones in various systems in response to stress factors outside the hypophysis. Now SST is known as a regulating peptide hormone, inhibiting several different hormones e.g. gastrin, glucagon, insulin, growth hormone and pancreatic polypeptide (Barbieri, et al., 2013, Bousquet, et al., 2012, Csaba, et al., 2001, Stengel, et al., 2013, Toumpanakis, et al., 2013).

Furthermore, it works as an endocrine and exocrine function modulator, which regulates differentiation and proliferation of normal and tumor cells (Csaba, et al., 2001, Ferjoux, et al., 2000).

There are two different types of the SST peptides SS-14 and SS-28, which differ in the number of amino acids, and SS-28 is a dimer of SS-14. These hormones are dominating at different sites. The predominant form is SS-14, which is produced in most of the peripheral organs and in the central nervous system, while SS-28 is mainly produced along the gastrointestinal tract by mucosal epithelial cells (Van Op den Bosch, et al., 2009). Further SS-14 is known to regulate the release of growth hormone secretion in hypothalamus, and indirectly the secretion of hormones in the thyroid (Yavropoulou, et al., 2013).

Theoretically, SST can be used to decrease the hormone production in patients with NET (Reubi, 1997), however, SST is not suitable for therapy, due to its short biological half-life (3 minutes). Several synthetic analogs have therefore been developed, e.g. octreotide and octreotate, which bind to the same receptors as SST but with different affinities (Grozinsky-Glasberg, et al., 2008, Grozinsky-Glasberg, et al., 2008).

1.2.1 Somatostatin receptors

SST interacts with cells by binding to and activation of G-protein-coupled somatostatin receptors (SSTRs), which are localized to the cell surface. There are basically five subtypes of SSTRs, but SSTR2 exists in two isoforms, SSTR2A and SSTR2B, and recently a human isoform of SSTR5 have been found (Barbieri, et al., 2013, Guillermet-Guibert, et al., 2005). SSTRs are transmembrane and have signaling, endocytosis and recycling functions, with different physiological effects. The SSTRs are differentially expressed in the central nervous and immune systems, in the pituitary, thyroid, and adrenal glands, and in pancreas, gut, and kidneys (Barbieri, et al., 2013). They form monomers, but have also shown homo- and hetero-dimerization which most likely alters the function of the receptors (Barbieri, et al., 2013, Terrillon, et al., 2004, Van Op den Bosch, et al., 2009).

The expression of SSTRs in tumors is complex. The receptor distribution depends on the tumor type, and differ between patients with similar tumor type and it might also differ between primary and secondary tumors (Forssell-Aronsson, et al., 2004). Furthermore, the affinity of SST analogs varies. The affinity is altered when the SST analogue is radiolabeled. Both ^{111}In-octreotide and ^{177}Lu-otreotate have highest affinity for SSTR2, followed by SSTR5, but DOTA-bound SST analogues have higher affinity to SSTR2 than DTPA-bound ones (Barbieri, et al., 2013, Esser, et al., 2006, Guillermet-Guibert, et al., 2005).

1.2.2 Internalization

When SST is bound to some SSTRs the complex might be internalized. In 1996, internalization and retention of ^{111}In-octreotide was demonstrated in human NETs (midgut carcinoid, gastric carcinoid and glucagonoma) (Andersson, et al., 1996), which previously only had been shown in vivo and in vitro for pituitary cells in rats, and in vitro in pancreatic acinar cells from guinea pigs, after injection of ^{125}I-SST (Morel, 1994, Viguerie, et al., 1987). This is essential for therapy, since internalization of the radionuclide might increase the retention in the cell and tumor, and also transport the radionuclide closer to the radiosensitive cell nucleus.

1.3 Radionuclide therapy of tumors

In radionuclide therapy, a radiopharmaceutical, consisting of a radiolabeled tumor-seeking agent, is administered to a patient and binds to a target on the cell surface, e.g. a receptor or an antigen. The radionuclide is then preferably internalized into the cell, to have a longer retention in the tumor cell and to be located closer to the cell nucleus, which is supposed to be the main radiation sensitive target of the cell (Hall, et al., 2006). Radionuclide therapy is becoming more established, as this type of radiation has large benefits; it is capable to reach spread tumors and tumor cells, also unknown metastases.

Since many years, ^{131}I as iodide is routinely used for treatment of differentiated thyroid cancer, ^{32}P as orthophosphate for therapy of polycythaemia and thrombocythaemia. ^{131}I-labeled meta-iodobenzylguanidine (MIBG) is used for treatment of pheochromocytoma, paraganglioma and neuroblastoma. Palliative treatments of bone metastases are also performed using, e.g., ^{89}Sr-chloride, ^{153}Sm-EDTMP, and ^{186}Re-HEDP (Carlsson, et al., 2002, Carlsson, et al., 2003). The last decade, therapy using ^{131}I- and ^{90}Y-labeled monoclonal antibodies, radioimmunotherapy (RIT), have been used against lymphoma, and ^{177}Lu- and ^{90}Y-labeled SST analogues against NET (Bodei, et al., 2011, Cremonesi, et al., 2006, Garkavij, et al., 2010, Kwekkeboom, et al., 2001, Sandstrom, et al., 2010, Sward, et al., 2010, van Essen, et al., 2009).

1.3.1 Problems and need for optimization of therapy using ^{177}Lu- octreotate

The main limiting organs in ^{177}Lu-octreotate therapy are the kidneys and bone marrow (Marks, et al., 2010). The tolerance doses, TDs, of these organs are not known (Van Binnebeek, et al., 2013), and TDs defined from external

beam radiotherapy are applied (Emami, et al., 1991). Initially the cumulative absorbed dose to the kidneys was limited to 23 Gy. Today, many clinics limit the cumulative absorbed dose to the kidneys to 27-28 Gy. Radiation induced kidney injury and renal functional impairment (radiation nephropathy) is a syndrome of chronic renal failure, which occur months or years after renal irradiation (Cohen, et al., 2001, Luxton, 1961) in contrast to acute radiation nephropathy which develops within a year after irradiation.

^{177}Lu-octreotate treatment is usually prescribed in a standard way, giving ca 7.4 GBq up to 4-6 times 2 months apart together with kidney blocking agents (Kwekkeboom, et al., 2005). The number of treatments given may in some clinics be defined from estimations of absorbed dose to kidneys and a assumed TD. Since the therapeutic effects of ^{177}Lu-octreotate therapy is limited, with a cure rate of less than 3%, there is a clear need for optimization of this treatment modality (Forssell-Aronsson, et al., 2013). Several ways for optimization could be used. One way is to optimize the treatment schedule and individualize treatment further. Another way is to reduce kidney uptake of ^{177}Lu to enlarge the therapeutic window.

1.4 Radiolabeled SST analogues

Initially in the 1980s, radioiodine-labeled SST analogues were tested for scintigraphy of SSTR expressing neuroendocrine NETs, but soon ^{111}In-labeled octreotide was developed (Ahlman, et al., 1994, Krenning, et al., 1989, Krenning, et al., 1992, Otte, et al., 1999). Today, the most commonly used radiolabeled SST analogues are based on octreotide or octreotate, which are closely related. The amino acid sequence of octreotide is D-Phe-Cys-Phe-D-Trp-Lys-Thr-Cys-Thr-ol, while for octreotate the third amino acid Phe (phenylalanine) and the terminal Thr-ol (threonine alcohol) are exchanged to Tyr (tyrosine) and Thr-OH (threonine hydroxyl), respectively (Figure 1.1).

For the radiopharmaceuticals based on SST analogues used for diagnosis and therapy today, the radionuclides (metal ions) are bound via a chelate, diethylene triamine pentaacetic acid (DTPA) or 1,4,7,10-tetraaza-cyclododecane-1,4,7,10-tetraacetic acid (DOTA) (Barbieri, et al., 2013).

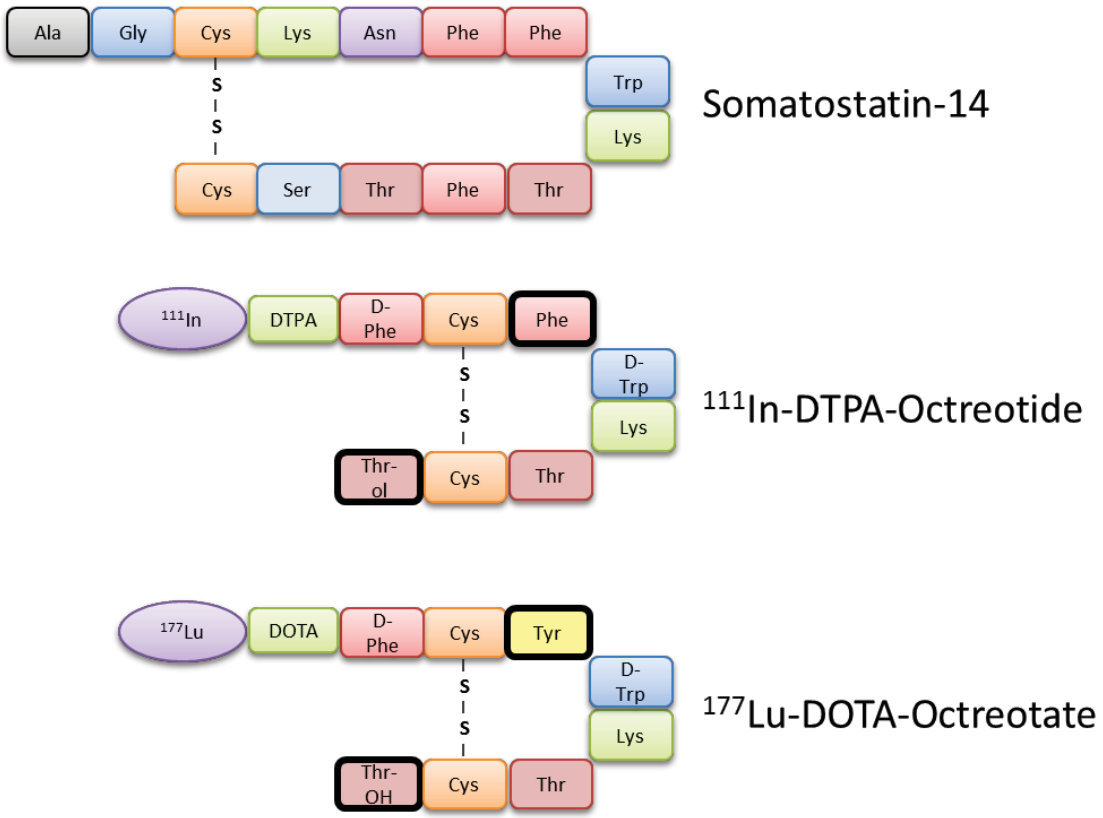

Figure 1-1 Native somatostatin-14 and two of the synthetic radiolabeled SST analogs developed. Octreotide and octreotate differ in amino acid sequence: Phe is exchanged with Tyr as third amino acid, and Thr-ol is exchanged with Thr-OH in octreotate compared with octreotide, marked with black borders. The radionuclides ^{111}In and ^{177}Lu are bound to the peptide via the chelates DTPA and DOTA, respectively. Redrawn from Barbieri, Bajetto et al. 2013 (Barbieri, et al., 2013)

^{111}In- DTPA- DPhe^{1}- octreotide

In [^{111}In-DTPA]-octreotide DTPA is the chelate that binds ^{111}In to octreotide,, Figure 1.1. The four amino acids Phe, D-Trp, Lys and Thr constitute the receptor binding part of the SST analogue. ^{111}In-octreotide has highest affinity to SSTR2 and SSTR5 (Barbieri, et al., 2013, Guillermet-Guibert, et al., 2005).

^{111}In decays by electron capture to stable ^{111}Cd (half-life of 2.8 days), and emits photons suitable for scintigraphy, Table 1.1.

^{111}In-octreotide (OctreoScan™, Mallinckrodt, Inc., St. Louis, MO, USA) is today routinely used for diagnostic scintigraphic imaging and evaluation before PRRT.

^{177}Lu- [DOTA^{0}- Tyr^{3}]- Octreotate

In [^{177}Lu-DOTA^{0}-Tyr^{3}]-Octreotate (^{177}Lu-octreotate) the chelating agent is DOTA, and the amino acids binding to the SSTR are Tyr, D-Trp, Lys and Thr Figure 1.1 (Barbieri, et al., 2013). Moreover, the octreotate has highest affinity for SSTR2 and SSTR5(Barbieri, et al., 2013).

^{177}Lu decays by β-decay, and emits electrons with an average kinetic energy of 147 keV per decay (ICRP107, 2008) (Table 1.1). The half-life of ^{177}Lu is 6.7 days. ^{177}Lu also emits photons, which enables scintigraphic imaging and dosimetric estimations.

^{177}Lu-octreotate is used for therapy in several clinics (Bodei, et al., 2011, Cremonesi, et al., 2006, Garkavij, et al., 2010, Sandstrom, et al., 2013, Sward, et al., 2010, van Essen, et al., 2009)

Table 1.1 Physical data for ^{111}In and ^{177}Lu (ICRP38, 1983). Values in brackets are the yields

Radio-nuclide	Half-life, daughter nuclide	Gamma energy [keV]	Beta, average energy [keV]	Characteristic X-ray energy [keV]	Auger electron energy [keV]	Conversion electron energy [keV]
^{111}In	**2.8 days**	**171 (90%)**		**23.0 (24%)**	**0.51 (191%)**	**145 (8%)**
	^{111}Cd (stable)	**245 (94%)**		**23.2 (44%)**	**2.6 (67%)**	**219 (5%)**
				26.1 (4%)	**3.2 (31%)**	
				26.1 (8%)	**3.6 (4%)**	
				26.6 (2%)	**19.2 (11%)**	
				22.3 (5%)		
^{177}Lu	**6.7 days,**	**113 (6%)**	**47 (12%)**	**7.9 (1%)**	**1.9 (19%)**	**48 (5%)**
	^{177}Hf (stable)	**208 (11%)**	**111 (9%)**	**9.0 (1%)**	**6.3 (5%)**	**102 (3%)**
			149 (79%)	**54.6 (2%)**	**8.1 (3%)**	**103 (3%)**
				55.8 (3%)		**111 (2%)**

1.5 Therapy using radiolabeled SST analogues

^{111}In-octreotide was initially tried for therapy of metastasized neuroendocrine tumors, resulting in modest tumor regression but symptom relief (Capello, et al., 2003, Fjalling, et al., 1996, Krenning, et al., 1999). ^{111}In is not a suitable radionuclide for therapy, due to the high photon emission and only very low energetic Auger and conversion electrons, but at that time no other radiolabeled SST analogue was available.

Nowadays, ^{177}Lu-octreotate and ^{90}Y-octreotide are used in PRRT of metastasized neuroendocrine tumors (Bodei, et al., 2011, Cremonesi, et al., 2006, Garkavij, et al., 2010, Sandstrom, et al., 2010, Sward, et al., 2010, van Essen, et al., 2009).

The β-emitting analogue ^{90}Y-octreotide, with relatively high energy electrons showed promising tumor regression (Paganelli, et al., 1999). However, the long range (mean of 12 mm) implies that it is best for large tumors. However, theabsorbed dose to bone marrow and bone marrow toxicity seems to be relatively high. The β-emitting analogue ^{177}Lu-octeotate, with medium energy electrons and shorter range (mean of 0.67 mm) are needed for small NETs and gives relatively low absorbed dose to kidneys and bone marrow.

1.6 Scintigraphy using gamma camera

Gamma camera scintigraphy is used to visualize the distribution of a radiopharmaceutical in the body. Briefly, photons emitted by the radionuclide from inside of the patient hits the detector in a small angle allowing the photons to pass through the collimator and interact with the scintillation crystal. From the crystal the signal will be transferred by the light guide and processed by the photomultiplier tubes, and the position of interaction and photon energy will be registered, Figure 1-2. The majority of the photons that are scattered or attenuated in the body will thus not be detected. Only emitted photons with a kinetic energy within, by the user specified, energy window will be registered. The signal is then presented as the number of photons counted in an image matrix with specified matrix size (Cherry, et al., 2012).

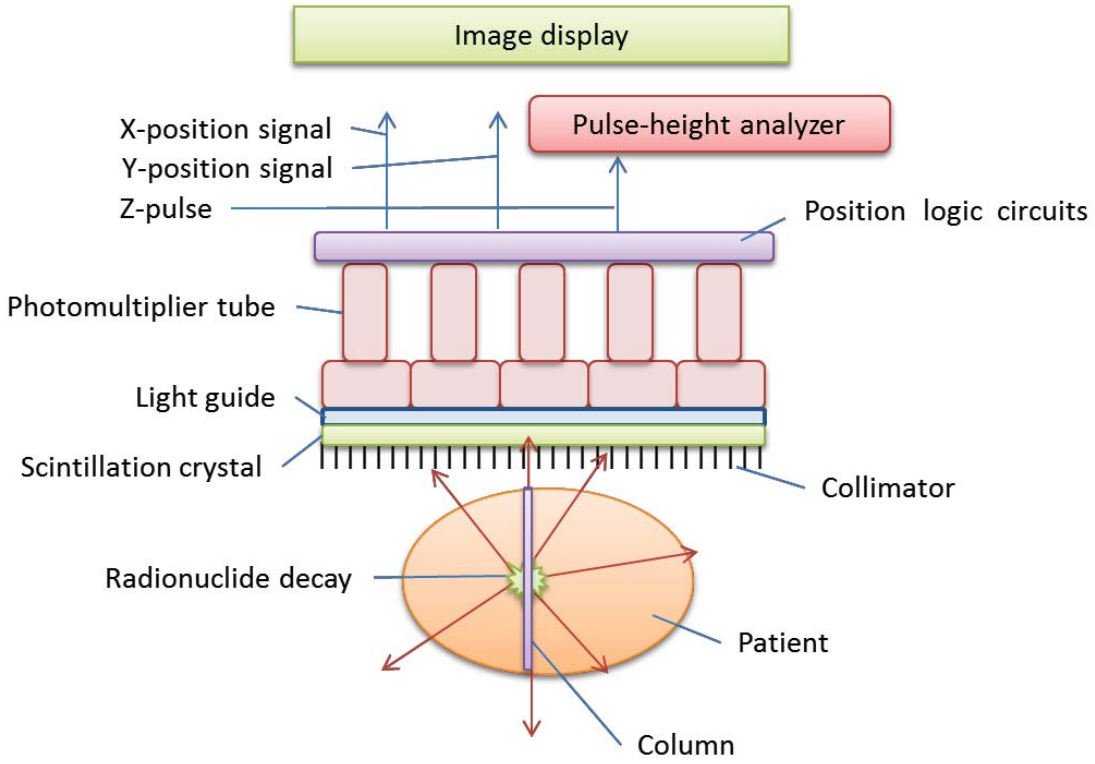

Figure 1-2 Schematic image of a gamma camera. Only photons that pass the collimator are detected

Factors affecting planar imaging

There are several factors that affect the pixel values in the scintigraphic image, when detailed analysis of radionuclide distribution in the body is performed. Some parameters are related to the gamma camera, such as sensitivity, spatial resolution, and acquisition parameters, e.g. energy window, acquisition time, matrix size and collimator. Other factors are related to the object, such as attenuation and scatter (partly also related to the detector), motion of the patient and organ, and presence of activity in over- and underlying tissues.

One important parameter is the choice of collimator for the actual application. This is based on a compromise between high sensitivity and high spatial resolution, due to the relation between septum thickness, hole diameter and the thickness of the collimator. Different parallel hole collimators are routinely used: Low Energy General Purpose (LEGP) and Low Energy High-Resolution (LEHR) (ore with smaller hole diameter or

thicker collimator) for ^{99m}Tc and different medium- and high energy collimators (with thicker septa to reduce penetration) for ^{111}In, and ^{131}I.

The sensitivity of the detector is determined by calibration of the gamma camera system, resulting in a measure of the number of counts detected per activity amount. To reduce the influence of photons that have interacted in the body, it is essential to choose a relatively small energy window around the photon energy to be measured. Scatter should be corrected for using either dual energy window settings or by measuring the effective attenuation coefficient in a broad beam set up (Hindorf, et al., 2010).

The matrix size should be chosen to achieve the best resolution for the application. The acquisition-time should be chosen in relation to acceptable image noise. If high amounts of activity is imaged, e.g. after radionuclide therapy, the effects of saturation of the system should be tested to minimize pulse pile-up (Cherry, et al., 2012).

1.6.1 Activity quantification

Conjugate view (CV) method

One of the first methods developed for absolute activity determination in an organ or tissue using planar scintigraphy was the geometric mean method, usually called the conjugate view (CV) method (Fleming, 1979, Thomas, et al., 1976). The CV method is still frequently used and considered to give good estimates of activity, e.g. according to Medical Internal Radiation Dose (MIRD) and EANM guide lines (Hindorf, et al., 2010, Lassmann, et al., 2011, Siegel, et al., 1999). The advantage of the method is that it takes into account the otherwise uncertain location (depth) of the organ, and the attenuation both in the organ and in surrounding tissues (Siegel, et al., 1999).

The CV method is based on two conjugate planar images, one anterior and one posterior image, either acquired with a camera with two camera heads or acquired consecutively, Figure 1-3.

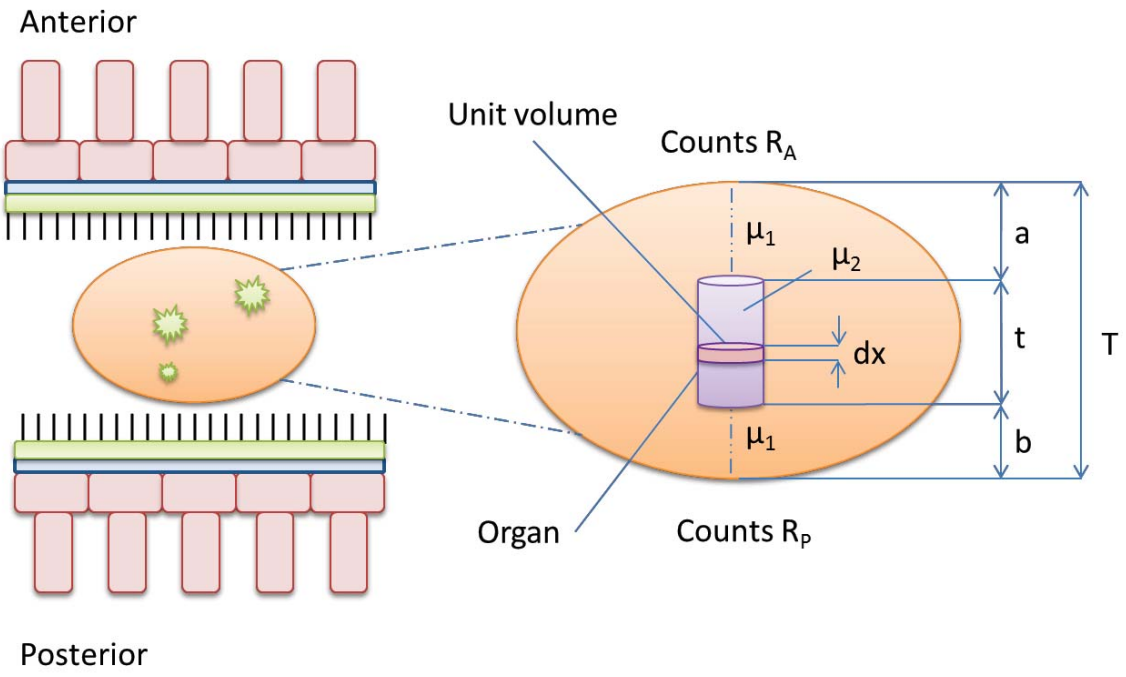

Figure 1-3 Schematic image showing the parameters used in the CV-method: the thickness T of the body and t of the organ, and μ_1 and μ_2 is the attenuation coefficient of the body tissue and organ, respectively.

The activity A (Bq), homogenously distributed in the organ of interest is calculated from counts from a region-of-interest (ROI) over the volume in the anterior, R_A, and posterior, R_P, images, Figure 1.4. Assuming linear attenuation coefficient μ_1, and μ_2, in the surrounded tissue and in the volume, respectively, and with the camera sensitivity factor k (cps/Bq), the counts from the volume in respective image can be written as (Fleming, 1979), with the distance a and b from the volume to the body surface, Figure 1-3.

$$\boldsymbol{R_A = ke^{-\mu_1 a} \int_0^t \frac{A}{t} e^{-\mu_2 x}\, dx = \frac{kAe^{-\mu_1 a}}{t\mu_2}[1 - e^{-\mu_2 t}]}, \qquad 1.1$$

and

$$\boldsymbol{R_P = \frac{kAe^{-\mu_1 b}}{t\mu_2}[1 - e^{-\mu_2 t}]}. \qquad 1.2$$

A geometrical mean of the opposite image count rates,

$$\sqrt{R_A R_P} = \frac{kAe^{-\mu_1(a+b)/2}}{t\mu_2}[1 - e^{-\mu_2 t}], \quad 1.3$$

If it is appropriate to assume that $\mu_1=\mu_2=\mu$ in the volume and the surrounding tissue, and setting $a+b+t = T$, the total activity, A (Bq), can be estimated by (Fleming, 1979),

$$A = \sqrt{\frac{R_A R_P}{e^{-\mu T}}} \frac{\frac{\mu t}{2}}{k \sinh\frac{\mu t}{2}}. \quad 1.4$$

The sensitivity of the gamma camera, k, is determined by measuring a planar source with a known activity of ^{177}Lu at different depths in a tissue equivalent phantom. From the signal *versus* depth curve the sensitivity and effective attenuation coefficient are determined from the intersection with the y-axis, and as the exponential coefficient, respectively (Fleming, 1979).

PA- method

If the organ is thin, with high activity and close to body surface, it might be better to calculate the activity using the count rate from one image (Hindorf, et al., 2010)

$$A = \frac{R}{e^{-\mu a}} \frac{\mu t}{k\,(1-e^{-\mu t})}. \quad 1.5$$

1.7 Dosimetry

According to the MIRD formalism the mean absorbed dose in the target tissue r_T, $\bar{D}_{r_T}$, can be calculated as (Bolch, et al., 2009)

$$\bar{D}_{r_T} = \sum_{r_S} \tilde{A}_{r_S} \times S_{(r_T \leftarrow r_S)}, \quad 1.6$$

where $\tilde{A}_{r_S}$ is the time integrated activity in the source tissue r_S, previously described as the cumulate activity (Loevinger, et al., 1988), and $S_{(r_T \leftarrow r_S)}$ is the mean absorbed dose to target per cumulated activity in source tissue. The summation includes contribution from all source tissues, including the target tissue. $\bar{D}_{r_T}$ depends on the biokinetics of the radiopharmaceutical, the physical decay properties of the radionuclide, and the geometry of the tissues in the body, both regarding size and location. $\tilde{A}_{r_S}$ is determined from biokinetic data obtained from scintigraphic images collected at several time-points after administration. Two or three time-points per exponential term in

the clearance curve of the organs have been recommended (Siegel, et al., 1999). The time integrated activity (or cumulated activity) can be estimated by calculating the area under the time-activity curve,

The S-value [Gy/Bq s] is given by

$$\boldsymbol{S}_{(r_T \leftarrow r_S)} = \frac{\sum_i E_i Y_i \phi_{(r_T \leftarrow r_S, E_i)}}{M_{r_T}}, \qquad 1.7$$

where E_i and Y_i are the mean energy and the number of the ith nuclear transitions per disintegration, respectively. The absorbed fraction, $\phi_{(r_T \leftarrow r_S, E_i)}$, is the fraction of energy E_i absorbed in the target r_T emitted from the source r_S (Bolch, et al., 2009, Stabin, et al., 2003).

1.8 Renal handling of ^{177}Lu- octreotate

1.8.1 The kidney and renal function

The kidney is a bean-shaped organ with a cortical shell surrounding the medulla. The functional unit of the kidney is the nephron, consisting of glomerulus and Bowman's capsule, proximal tubule, loop of Henle, and distal tubule, which transports the urine via collecting ducts to the renal pelvis (Figure 1-4) (Taal, et al., 2012).

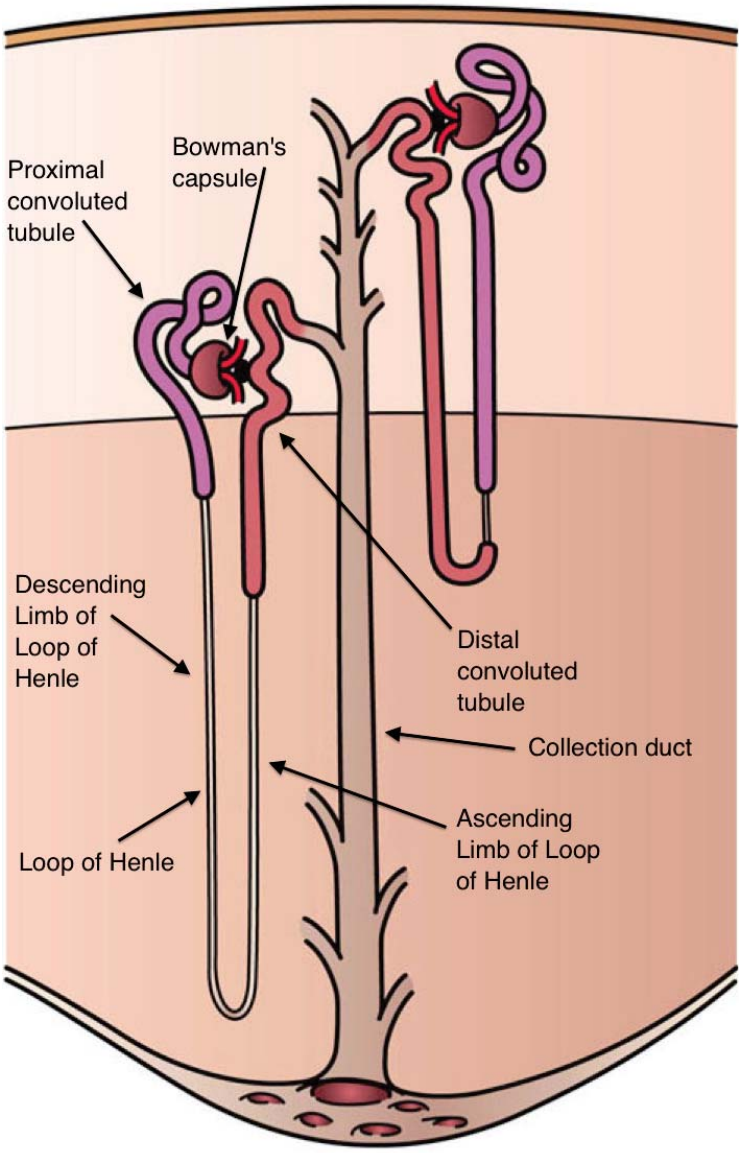

Figure 1-4 Schematic anatomical image of a section thorough a nephron (outer cortex and part of the medulla) in the kidney. The image is in the public domain.

The glomerulus consists of vascular bundles inside the Bowman's capsule, where afferent (incoming) blood is filtrated over the thin capillary walls, i.e the glomerulus barrier, into the capsule. The glomerular barrier is a highly complex membrane, allowing large amounts of water and small to middle sized (less than ca 100 Å) molecules to pass and be primary urine, while large molecules are restricted. There is also a selection on charge, and molecules of negative charge will be less filtered although the size is small enough. Non filtered molecules will return to the blood system via the efferent arterioles.

Each nephron will then continue from the Bowman's capsule into a winding tube of tubular cells. In first part, the proximal tubule, about two thirds (66%)

of the water and electrolytes and almost all nutrients will be reabsorbed from the primary urine. The tube makes a turn in the loop of Henle and thereafter continues by the distal tubule. Along the whole tubular system reabsorption and secretion may occur, and the remaining final urine will be collected in collecting ducts and thereafter transported to the kidney pelvis and reach the urinary bladder via ureters.

The main function of the renal system is to maintain the homeostasis, i.e., holding the body and cells in a stable environment, especially by regulating the urine and fluid balance, the salt and mineral and acidity (pH) levels in the blood and other fluids in the body. The production of hormones and D-vitamin is also important (Taal, et al., 2012). About 180 liter per day (125ml/min) of blood plasma flows through the kidneys, where amino acids, protein and peptides, mineral ions such as sodium (Na^+), potassium (K^+), chloride (Cl^-), magnesium (Mg^+) are filtered. Reabsorption and secretion is performed by diffusion (movement from high to low concentration), osmosis (water molecule diffusion), and passive (none energy consuming) or active (energy consuming) transporters in the tubular cells (Haraldsson, et al., 2008, Taal, et al., 2012).

1.8.2 Retention of ^{177}Lu in kidneys

Radiolabeled small peptides are most often excreted to a high extent by the kidneys. Radiolabeled SST analogs are filtered and to some degree reabsorbed in the kidneys, especially in the tubular cells, which may result in high absorbed dose to the kidneys and, nephrotoxicity (Melis, et al., 2005, Vegt, et al., 2010). The retention mechanisms are not fully understood and several ways for the radiopharmaceuticals to enter the tubular cells are suggested, e.g., via passive diffusion, pinocytosis, aminoacid/oligopeptide transporters and via receptor mediated endocytosis (megalin/cubilin receptors and SSTRs) (Forssell-Aronsson, et al., 2013, Vegt, et al., 2010).

SSTRs are expressed in vasa recta (capillaries surrounding loop of Henle), tubuli and in the glomeruli of the kidneys (Rolleman, et al., 2007), but the importance of SSTRs for ^{177}Lu retention in kidneys is not fully known.

The megalin-cubilin receptors can separately bind to peptides and proteins and also interact. Megalin is necessary for the internalization of some molecules (e.g. octreotide and octreotate) (Christensen, et al., 2001, 2002, Christensen, et al., 1998, Christensen, et al., 2009, de Jong, et al., 2005, Weyer, et al., 2013).

There is also a low uptake via direct tubular secretion and peritubular absorption by organic anion-, cation- or oligopeptide transporters.It has been suggested that ^{111}In-octreotide enters the anion pathway, either from the plasma or from the tubular lumen (Stahl, et al., 2007).

After degradation of the radiopharmacutical in the tubular cells into amino acids and residual radioconjugates, the amino acids are recycled into the plasma fluid, while the radioconjugates seem to be unable to pass through the lysosome membrane, and are kept in the cells (Christensen, et al., 2009, Haraldsson, 2010, Vegt, et al., 2010).

1.8.3 Measuring renal function

Glomerular filtration rate (GFR) is the main parameter used to measure renal function. GFR gives a measure of the number of functioning nephrons in the kidney and can be assessed by several methods. Per definition GFR is the volume of blood filtered by the glomerular barrier per unit time and there are several molecules that can be used to estimate GFR.

There are also other parameters indicating altered renal function, not based on GFR. Of importance for radionuclide therapy is tubular function.

Exogenous markers and methods, including scintigraphy

GFR

The golden standard and the most accurate GFR estimate is to measure the blood clearance of inulin, which is neither reabsorbed nor secreted by the tubular cells, making it an ideal marker for GFR. It is, however, rarely used due to clinical limitations (Lamb, et al., 2014).

Instead, blood clearance of other molecules are used, where these molecules are filtered through the glomeruli, without significant reabsorption or secretion into the tubules and low binding to plasma proteins: iohexol (Krutzen, et al., 1984), ^{51}Cr-EDTA, ethylenediamine tetraacetic acid, and ^{99m}Tc-DTPA (Daniel, et al., 1999).

^{99m}Tc-DTPA is cleared via glomerular filtration and has no or minor reabsorption or secretion. It has a rapid blood clearance of 20% in the first passage and the biological half-life ($T_{1/2}$) is 2.5 h in humans (Daniel, et al., 1999). It can be studied by dynamic scintigraphy, due to the 140 keV gamma rays of ^{99m}Tc, and the uptake and clearance from the plasma is directly related to GFR (Osman, et al., 2014). Plasma protein bound DTPA (less that 5%) is not filtered through the glomeruli and results in a too low GFR estimate.

Tubular function

^{99m}Tc-MAG3, mercaptoacetyltriglycine, is primarily secreted into the tubules (90%) with low glomerular filtration (10%). It is taken up mainly in the proximal tubule cells via active transport sites and is excreted quickly to the bladder. ^{99m}Tc-MAG3 is not used for GFR estimation, but primarily for localization of non-functional regions of the kidneys via scintigraphy.

^{99m}Tc-DMSA is used for imaging of dysfunctional areas in the kidneys, especially in the kidney cortex. It is taken up by the proximal tubular cells from the blood, but is also to some extent filtered by the glomeruli and reabsorbed or bound to plasma proteins (de Lange, et al., 1989, Peters, et al., 1988). The cortex/medulla ratio for DMSA is 22:1, and after 2-3 h 40-50% of the administered activity is located in the cortex. (Daniel, et al., 1999, Freitas, et al., 1996). Studies show that megalin/cubilin receptors are essential for the uptake of ^{99m}Tc-DMSA by the tubular cells (Weyer, et al., 2013).

Endogenous markers and methods

Creatinine is a rest product after muscle metabolism of creatine. It is filtered through the kidneys and to a major extent excreted. An elevated plasma creatinine value is an indicator of renal impairment by reduced GFR. However, plasma creatinine level is not only influenced by GFR, it is also dependent on nutritional intake, muscle mass, body weight, age and gender and is therefore a weak marker for GFR (Slocum, et al., 2012).

Cystatin C is constantly produced by all cells with cell nucleus in the body and is filtered by glomerulus and excreted by urine. Studies have shown that serum and urinary cystatin C have potential as early diagnostic markers for acute kidney failure, and it is discussed whether to use cystatin C rather than creatinine for estimation of GFR (Bagshaw, et al., 2010, Carbonnel, et al., 2008). Also the cystatin C level seems to be modified by age, sex, muscle mass, obesity, smoking status, thyroid function, inflammation, and malignancy (Bagshaw, et al., 2010).

Urea, $CO(NH_2)_2$, is a byproduct after protein degradation in the liver. It constitutes the major form of nitrogen waste in the body, and is to 90% excreted via the kidneys. Reabsorption of urea via urea transporters occurs in the proximal nephron, up to 40% of the filtered urea, and in a regulated way in the distal nephron (Fenton, et al., 2007). An elevated urea level in the blood is an indicator for renal impairment.

Other important indicators for renal function are the hemoglobin value, which is lower in patients with renal impairment, the potassium, sodium, calcium,

and the phosphate blood levels which become altered when the kidneys are not working normally, and protein leakage into urine (Taal, et al., 2012).

1.8.4 Methods to reduce kidney uptake of ^{177}Lu

Lysine and Arginine

Positively charged amino acids infused when ^{177}Lu-octreotate is given may reduce the uptake of radiolabeled peptides but may give side effects such as vomiting, metabolic changes and hyperosmolarity (Rolleman, et al., 2008, Rolleman, et al., 2003). Lysine and arginine are today given to patients with NET treated with ^{177}Lu-octreotate and reduce the kidney uptake by 20-40% (Bernard, et al., 1997, Melis, et al., 2007, Rolleman, et al., 2003).

DMSA

Although lower uptake of ^{177}Lu-octreotate is seen when using amino acid blockage, other molecules might reduce it even more. The mechanisms of kidney handling of DMSA are not fully known. DMSA is both reabsorbed and secreted by the tubules, known to be mediated by megalin-cubilin receptors as mentioned above (Weyer, et al., 2013). Blocking those pathways for ^{177}Lu-octreotate might improve the kidney blocking. Preliminary studies have shown that DMSA injection prior to ^{177}Lu-octreotate increased the kidney uptake, whereas administrated 1h after ^{177}Lu-octreotate reduced the renal uptake (Moorin, et al., 2007).

Other agents

New renal blocking agents are investigated such as using the gelatin Gelofusine and albumin fragments (Rolleman, et al., 2010, Vegt, et al., 2010).

2 AIMS

Therapy with ^{177}Lu-octreotate for patients with neuroendocrine tumors shows promising results, but few patients undergo complete remission with the treatment protocols used today. The overall aim of this thesis was to obtain more knowledge on pharmacokinetics, dosimetry and kidney toxicity, and to find ways to optimize therapy in order to widen the therapeutic window.

The specific aims of thesis were to

- Determine the pharmacokinetics of ^{177}Lu-octreotate in patients with NET (Papers I and II).

- Determine the dosimetry of ^{177}Lu-octreotate in kidneys, liver, spleen, red marrow and tumor tissues in patients with NET (Papers I and II).

- Determine radiobiological effects on kidneys in a mouse model after exposure to ^{177}Lu-octreotate, using various methods including analysis of potential biomarkers in blood and urine, scintigraphy and with RNA transcript analysis (Paper III).

- Investigate the potential of DMSA, either alone or in combination with lysine, for blocking of the kidney uptake after i.v. injection with ^{111}In-octreotide in mice (Paper IV).

3 MATERIAL AND METHODS

3.1 Activity determination

3.1.1 Scintigraphy of patients (Papers I, II)

Anterior and posterior whole body images were acquired with a Picker IRIX system (Marconi, Philips, Holland) or a Millennium VG Hawkeye system (General Electric Medical Systems, Milwaukee WI, USA), equipped with medium energy parallel-hole collimators, at one hour, and 1, 2, and 7 days after ^{177}Lu-octreotate administration. The gamma cameras were set to collect signals from the 208-keV photon peak of ^{177}Lu, with a 20% energy-window.

SPECT/CT was performed at day one over the kidney region. The computed tomography (CT) images were only used for determination of the thickness and volume of organs and to outline the body surface, and the single-photon emission computed tomography (SPECT) images only localization of tissues with high ^{177}Lu activity concentration close to the organs/tissues of interest.

Processing and image analysis were carried out on a GENIE Xeleris workstation (General Electric Medical Systems, Milwaukee, WI, USA).

The sensitivity, k, and the effective linear attenuation coefficient, μ, for ^{177}Lu were determined for the gamma cameras using a ^{177}Lu filled planar source and a polystyrene phantom with a density of 1.05 g/cm^3 (Fleming, 1979).

The ^{177}Lu activity in whole body, kidneys, liver, spleen and tumors, was determined from the planar images. Regions of interest (ROIs) were drawn in the image where the organ/tissue was best visualized (usually at day 1 or 2). The ROIs were then mirrored onto corresponding opposite image, and these two ROIs were then applied for in all images of that patient and that treatment cycle. If overlapping tissues contain high amount of ^{177}Lu, small ROIs were drawn over only a part of the organ, without overlapping activity, and the total number of counts in the organ was estimated, assuming similar counts per pixel within the organ.

For background subtraction, a small circular ROI was placed adjacent to, for kidneys, and in the very vicinity for liver, spleen and tumor. (Buijs, et al., 1998, Norrgren, et al., 2003).

The activity, *A*, was determined according to the CV method, and for kidneys also the PA method.

3.1.2 Scintigraphy of mice (Paper III)

Linearity (for the activity range of the study) and homogeneity of the camera was measured and accepted. A calibration syringe was included in all images.

^{99m}Tc-DTPA and ^{99m}Tc-DMSA scintigraphy of mice were performed using a single headed gamma camera ADACT 210 (ADAC Laboratories A/S, Aalborg, Denmark). Energy window was centered over the 140 keV photon peak. After i.v. injection of 55 MBq ^{99m}Tc-DTPA, images were acquired every 5th minute between 2.5 and 33.5 minutes after injection. Two days later the mice were i.v. injected with 40 MBq ^{99m}Tc-DMSA, and a static image was acquired 3 h after injection.

ImageJ software (Schneider, et al., 2012) was used for image processing.

3.1.3 Activity in syringes (Papers I- IV)

Activity in syringes was determined before and after administration of ^{177}Lu-octreotate using an ionization chamber (Capintec CRC®-120, Scanflex Medical AB, New Jersey, USA) (Papers I, II).

Activity in syringes was determined before and after injection of ^{177}Lu-octreotate, and ^{111}In-octreotide with another ionization chamber (Capintec CRC®-15, Capintec, IA, USA) (Papers III, IV).

Activity in syringes was determined before and after injection of ^{99m}Tc-DTPA, and ^{99m}Tc-DMSA, with a third ionization chamber (Capintec CRC®W-120, Scanflex Medical AB, NJ, USA) (Paper III).

3.1.4 Activity in tissue samples (Paper IV)

Calibration of the gamma counter was made using a linear approximation and the efficiency of the counter was calculated.

Activity in tissue samples were measured with the calibrated gamma counter (3” NaI(Tl) crystal, Wizard 1480, Wallac, Finland). Corrections were done for background and dead time.

The activity concentration per gram of tissue per injected activity (%IA/g) was determined as:

$$C_{tissue} = \frac{A_{tissue}/m_{tissue}}{A_{injected}} * 100, (\%IA/g) \quad 3.1$$

where A_{tissue} and m_{tissue} is the activity and mass of the sample, respectively, and $A_{injected}$ the activity injected, A_{tissue} was decay corrected to the time of injection.

3.2 Radiopharmaceuticals and chemicals

3.2.1 ^{177}Lu- octreotate (Papers I, II and III)

^{177}Lu-octreotate was produced according to instructions by the manufacturer (I.D.B. Holland, Baarle-Nassau, Netherlands). More than 99% of ^{177}Lu was peptide-bound, determined by instant thin-layer chromatography.

3.2.2 ^{99m}Tc- DTPA (Paper III)

^{99m}Tc-DTPA (diethylene-triaminepenta-acetate) (Covidien, Dublin, Ireland), was produced according to the instructions by the manufacturer.

3.2.3 ^{99m}Tc- DMSA (Paper III)

^{99m}Tc-DMSA (dimercaptosuccinic acid) (Covidien, Dublin, Ireland), was produced according to the instructions by the manufacturer.

3.2.4 ^{111}In- octreotide (Paper IV)

^{111}In-octreotide (Octreoscan™, Covidien, Dublin, Ireland) was produced according to instructions by the manufacturer, thereafter diluted to the right concentrations.

3.2.5 Chemicals (Paper IV)

DMSA was obtained by Covidien (Dublin, Ireland), and L-lysine by Sigma-Aldrich (St. Louis, MO, USA).

3.3 Patients

Paper I and II

A total of 33 patients with disseminated NET, 13 women and 20 men, 40-80 years old were included in the study. All patients had undergone surgery.

Prior to ^{177}Lu-octreotate therapies some of the patient underwent other treatments, e.g. hepatic artery embolization, liver transplantation (four patients), SST analogs, and chemotherapy.

For each patient individually license for treatment with ^{177}Lu-octreotate was received from Swedish National Medical Products Agency. Ethical approval was given for evaluation of scintigraphic imaging by Regionala etikprövningsnämnden i Göteborg.

3.4 Patient studies (Papers I- II)

Patients were treated with 3.4 to 8.2 GBq ^{177}Lu-octreotate up to five times (treatment cycles, TCs). To reduce kidney uptake the patients received infusion with lysine and arginine in saline solution starting 30 minutes before administration of ^{177}Lu-octreotate.

Scintigraphy was performed, as described above. The ^{177}Lu activity was determined in whole body, kidneys, liver, spleen, and tumors (liver metastases (LM), bone metastases (BM) and other metastases (OM)). The ^{177}Lu activity was also determined in the following body regions: thorax, abdomen, head and extremities.

The mean absorbed dose per administered activity was determined for kidneys (Paper I), and liver, spleen, tumors and bone marrow (Paper II).

Kidney

The mean absorbed dose per administered activity was determined for each kidney in three ways:

(1) by the CV method with patient-specific organ sizes, (2) by the PA method with patient-specific organ sizes, and (4) by the CV method with standard organ sizes. Furthermore, the importance of each measurement point was determined using the first method and with reduced number of image time points.

Liver

The mean absorbed dose per administered activity was determined for liver by the CV method using a scaled abdominal thickness and liver thickness (Fleming, 1979), and with standard organ sizes: 1800 g for male and 1400 g for female (Valentin, 2002).

Spleen
The mean absorbed dose per administered activity was determined for spleen by the CV method using standard mass of the spleen: 150 g for male and 130 g for female (Valentin, 2002).

Bone marrow
The mean absorbed dose per administered activity was determined for red bone marrow based on whole body activity, using three different ROIs: thorax, abdomen, head and extremities, and the activity in liver, spleen and kidneys.

A scaled attenuation coefficient was used for the ^{177}Lu content in thorax region, according to

$$\boldsymbol{\mu_{scaled}} = \frac{\boldsymbol{T_{Lung}}}{\boldsymbol{T_{Chest}}} * \left(\frac{\boldsymbol{\mu}}{\boldsymbol{\rho}}\right)_{\boldsymbol{lung}} \boldsymbol{\rho_{lung}} + \frac{\boldsymbol{T_{Chest\ wall}}}{\boldsymbol{T_{chest}}} * \left(\frac{\boldsymbol{\mu}}{\boldsymbol{\rho}}\right)_{\boldsymbol{skeleton}} \boldsymbol{\rho_{skeleton}}, \qquad 3.2$$

where T_x is the thickness for reference man (x = the lung, chest and chest wall), and $\left(\frac{\mu}{\rho}\right)_x$ is the linear attenuation coefficient and ρ_x the dencity for lung and skeleton.

Tumor
The mean absorbed dose per administered activity was determined for LM, BM and OM with estimated volume (mass) of the tumors mean full width at half maximum (FWHM) from images day 1 and 2, assuming spherical or ellipsoidal shape.

3.5 Animals (Papers III- IV)

C57BL/6N female mice were obtained from Charles River (Salzfeld, Germany). The mice were 5-6 weeks old in paper III and 8 weeks old in paper IV. Food and water were given ad libitum.

3.6 Animal studies

Paper III
Mice were i.v. injected with 30-150 MBq ^{177}Lu-octreotate. Control mice were injected with saline solution. After 4, 8, or 12 months, some mice were subjected to scintigraphic analysis using ^{99m}Tc-DTPA and ^{99m}Tc-DMSA, while other mice were killed, and blood samples collected for further

analysis, and the kidneys excised for analysis by transcriptional microarray and histology.

The experimental protocol was approved by the Ethical Committee on Animal Experiments in Gothenburg, Sweden.

Paper IV

Mice were i.v. injected in the tail vein with 3.5 MBq ^{111}In-octreotide. Some mice were also injected with various amounts of DMSA, lysine or the combination of the two (DMSA+lysine) 0-2 h before injection of ^{111}In-octreotide. The mice were killed 24 hours after injection, and the ^{111}In concentration was determined in blood, kidneys, and other normal tissues.

The experimental protocol was approved by the Ethics committee on Animal Research in Gothenburg, Sweden.

3.7 Dosimetry (Papers I- III)

Throughout paper I and parts of paper II, for all organs but bone marrow and tumors, the S-value was exchanged with the mean energy of the beta decay for ^{177}Lu, the absorbed fraction was set to unity (Siegel, et al., 1994), and the mass will be approximated as ellipsoids or spheres using image data from CT. In paper II comparable dose factor (DF) replace the S-values (Stabin, et al., 2011).

Monoexponential curves were fitted to each time-activity data set, from where the effective decay constant, λ_{eff}, and the activity, A_0, at time 0 was determined.

The cumulated activity $\tilde{A} = \int_0^\infty A_0 e^{-\lambda_{eff} \cdot t} dt = \frac{A_0}{\lambda_{eff}}$ was then calculated for all organs and tissues of interest.

Paper I and II

Kidney

The mean absorbed dose to each organ was determined according to MIRD formalism (Loevinger, et al., 1988)

$$\overline{\boldsymbol{D}}_{\boldsymbol{kidney}} = \tilde{\boldsymbol{A}}_{\boldsymbol{kidney}} \times \sum_{\boldsymbol{i}} \boldsymbol{n_i E_i} \times \boldsymbol{\phi_i} / \boldsymbol{m_{kidney}}, \qquad 3.3$$

where $\tilde{A}_x$ was the cumulated activity in organ *x*, the energy emitted by electrons per decay, $\sum_i n_i E_i$, was assumed to be 147 keV for ^{177}Lu (Guillermet-Guibert, et al., 2005, ICRP38, 1983, ICRP107, 2008), the absorbed fraction, ϕ_i, was set to 1 and m_x was the mass of the kidney (Larsson, et al., 2012).

For more details, see paper I.

Liver and spleen

The mean absorbed dose was calculated with the same assumptions as for the kidneys.

For more details, see paper II.

Bone marrow

The mean absorbed dose to red bone marrow (RM) was estimated using

$$\overline{\boldsymbol{D}}_{\boldsymbol{RM}} = \widetilde{\boldsymbol{A}}_{\boldsymbol{RB}} * \boldsymbol{DF}_{(\boldsymbol{RM}\leftarrow\boldsymbol{RB})} + \sum_{\boldsymbol{organ}} \widetilde{\boldsymbol{A}}_{\boldsymbol{organ}} * \boldsymbol{DF}_{(\boldsymbol{RM}\leftarrow\boldsymbol{R}_{\boldsymbol{organ}})}, \quad 3.4$$

where the dose factor, $DF_{(B\leftarrow A)}$, the fraction of the energy emitted from organ *A* that will be deposited in organ *B*. The dose factors for liver, spleen, kidney were obtained from RADAR webpage (Stabin, et al., 2011), while the dose factors for the remainder of the body to red marrow was determined according to

$$\boldsymbol{DF}_{(\boldsymbol{RM}\leftarrow\boldsymbol{RB})} = \boldsymbol{DF}_{(\boldsymbol{RM}\leftarrow\boldsymbol{TB})} \frac{\boldsymbol{m}_{\boldsymbol{TB}}}{\boldsymbol{m}_{\boldsymbol{RB}}} - \sum_{\boldsymbol{organ}} \boldsymbol{DF}_{(\boldsymbol{RM}\leftarrow\boldsymbol{R}_{\boldsymbol{organ}})} \frac{\boldsymbol{m}_{\boldsymbol{organ}}}{\boldsymbol{m}_{\boldsymbol{RB}}}, \quad 3.5$$

where $DF_{(RM\leftarrow R_{organ})}$ is the dose factor for each organ (spleen, liver and kidneys) (Stabin, et al., 2001) and m_x the mass for respective organ/tissue.

For more details, see papers I and II.

Tumor

The mean absorbed dose to tumors was estimated using dose factors, for spherical tumors, determined according to $DF = 0.023 {m_{tumour}}^{-0.991}$, where m_{tumor} is the tumor mass in gram (Stabin, et al., 2011). No contribution from cross dose was included in the tumor dosimetry.

For more details, see paper II.

Paper III

The cumulated activity of ^{177}Lu was calculated from biodistribution data on C57BL/6N mice after ^{177}Lu-octreotate administration (unpublished data). The absorbed fraction was set to 0.93 (Miller, et al., 2005). Only contribution from electrons was included in the mean absorbed dose.The estimated absorbed dose to the kidneys in paper III was calculated according to the MIRD formalism according to equation 3.3, assuming a homogeneous activity distribution.

4 RESULTS

4.1 Patient studies (Paper I- II)

Paper I

The data for kidneys in the 33 patients administered with ^{177}Lu-octreotate demonstrated that there was a large spread among patients both in time-activity curve pattern and in the mean absorbed dose to the kidneys, either estimated with the CV-method or with the PA-method, and with patient specific or standard organ sizes.

The time-activity curve had the maximum value either at the first time-point or after 1 or 2 days after ^{177}Lu-octreotate administration. Moreover, inter individual variation in mean absorbed dose to the kidneys per administered activity was 0.33-2.4 Gy/GBq (mean value 0.80 Gy/GBq) based on the CV method (Figure 4.1). Corresponding value for the first treatment cycle was 0.38-1.7 Gy/GBq (mean value 0.84 Gy/GBq). Corresponding data from all treatment cycles using the PA-method was 0.29-1.2 Gy/GBq (mean value 0.60 Gy/GBq). The correlation between mean absorbed dose to the kidneys per administered activity determined by the two methods was statistically significant, $p<0.001$.

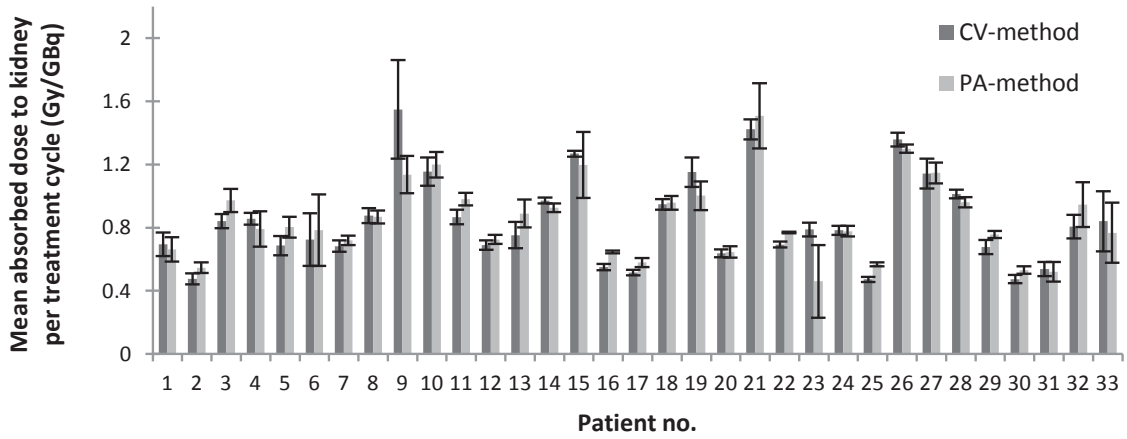

Figure 4-1 Mean absorbed dose to kidneys per administered activity per treatment cycle in patients treated with ^{177}Lu-octreotate, estimated with CV- or PA-method.

There was no trend towards higher or lower mean absorbed dose per administered activity for kidneys with increased number of treatment cycles. The mean deviation of all subsequent kidney doses from the first-fraction dose was only 1% (range: -31% to +47%) for the right kidney and only 5% (range: -26% to +93%) for the left kidney (Figure 4.2).

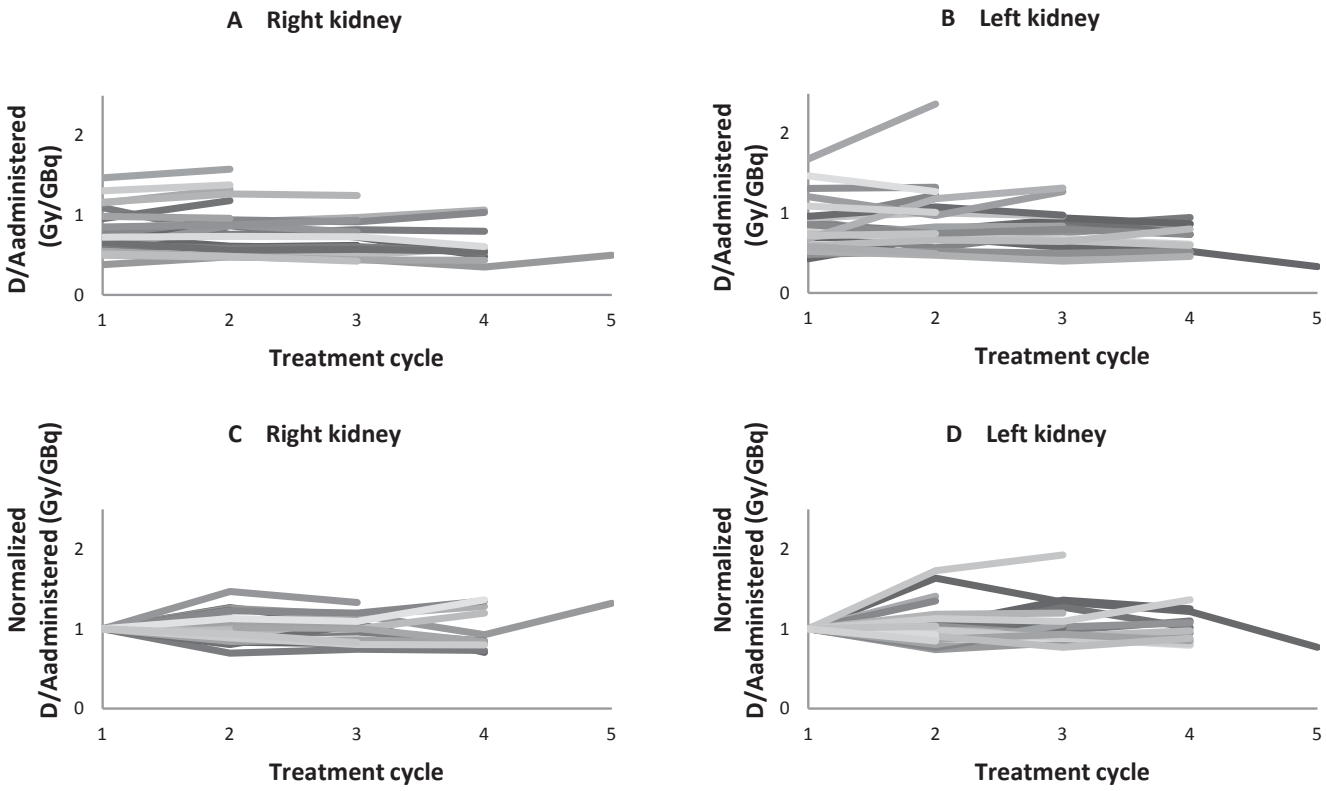

Figure 4-2 Mean absorbed dose to kidneys per administered activity for all patients in A) right and B) left kidney. C) and D) show corresponding data normalized to the value for first treatment cycle, respectively.

Estimation of the mean absorbed dose with the CV-method with standard organ sizes leads to a 50% underestimation for patients with small kidneys (<100 g) and a 50% overestimation for patients with large kidneys (>150 g) compared with corresponding values using patient-specific kidney volumes (masses).

Based on our findings the number of time points had significant influence on estimation of mean absorbed dose. If data was excluded for day 7, the most

important of the time-points used, the variation was up to a factor of 2.3, compared with when all data was included.

Paper II

There was a large variation in mean absorbed dose per administered activity to normal tissues and tumors, between patients and between treatment cycles (TCs) in the same patient.

Generally the time-activity curves showed no uptake phase for the liver as seen for the kidneys; spleen differed from the liver, with a maximum at day 1, and in a few cases at day 2. Hence, between patients there was a maximal difference in activity content per administrated activity, of a factor 11 and 20 for liver and spleen, respectively. The time-activity curve pattern for whole body (WB) did not differ between patients, and the mean percentile activity per administrated activity at time-point 0 h in WB was 87% ± 14%, and the mean retention time was 40 ± 16 h (SD).

Paper II presents the mean absorbed dose per administered activity, $D/A_{administered}$, to the liver without metastases, spleen, red marrow and kidney, from totally 43 treatments. The average value for liver was 0.19 Gy/GBq (0.047-0.54 Gy/GBq), for spleen 1.2 Gy/GBq (0.28-4.4 Gy/GBq), for red marrow 0.034 Gy/GBq (0.010-0.093), compared to kidney average of 0.80 Gy/GBq, Figure 4.3. When including the liver metastases in the mean absorbed dose for liver the average dose became 0.42 Gy/GBq (0.050-2.4 Gy/GBq).

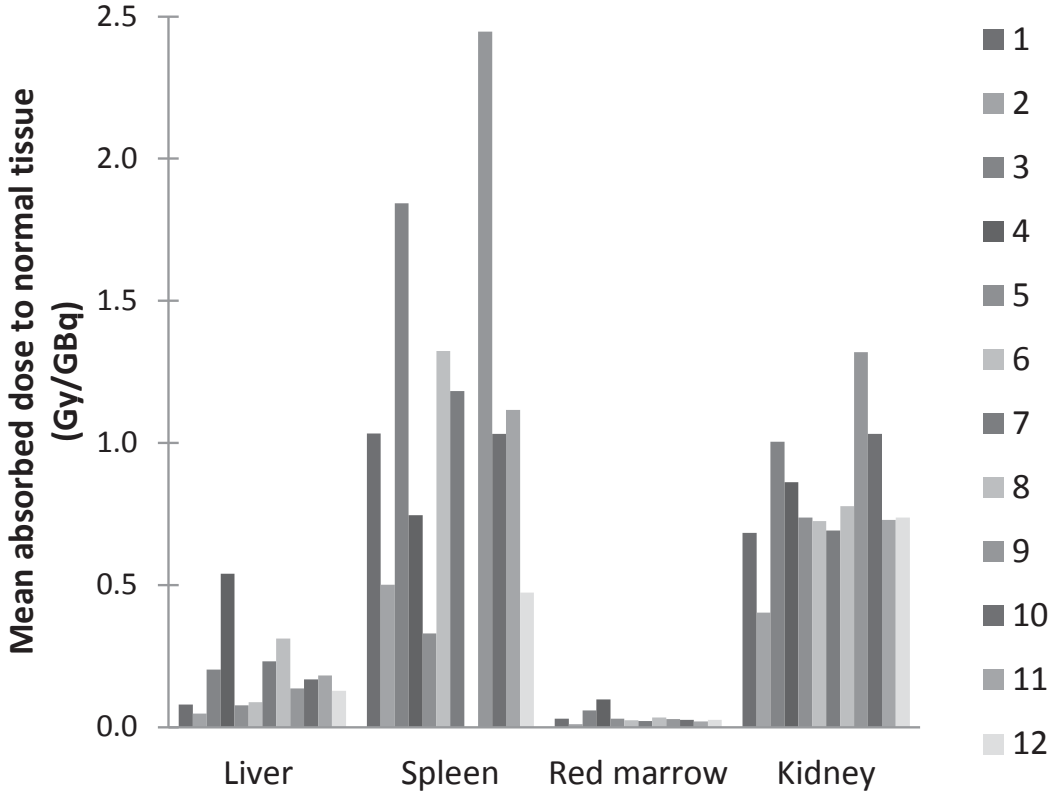

Figure 4-3 Mean absorbed dose per administrated activity for liver, spleen, red marrow and kidney, first treatment cycle, for 12 patients. Kidneys are presented as an average of the right and left mean absorbed kidney dose.

When including all treatment cycles for each patient, the total mean absorbed dose for the liver was 0.70-14 Gy without metastases, and 1.2-49 Gy with metastases, for spleen 8.6-52 Gy, and for the red marrow 0.40-2.2 Gy.

The time-activity curve pattern for tumors generally looked the same for LM and BM with an uptake phase (max) at day 1 or 2 after ^{177}Lu-octreotate administration, while for OM (soft tissue and lymph node metastases) no uptake phase was seen in some of the patients. The uptake per administrated activity became lower with treatment cycle but the curve pattern was usually similar throughout all treatment cycles.

The mean absorbed dose to tumor per administered activity was 7.1 Gy/GBq (0.43-20 Gy/GBq) to LM, 4.1 Gy/GBq (1.3-12 Gy/GBq) to BM and 3.4 Gy/GBq (0.47-14 Gy/GBq) to OM.

4.2 Animal studies (Papers III- IV)

Paper III

The absorbed dose to the kidneys in C57BL/6N mice injected with 30, 60, 90, 120, and 150 MBq ^{177}Lu-octreotate was 19, 34, 45, 52, and 55 Gy, which corresponds with mean absorbed dose per administered activity of 0.62 to 0.36 Gy/MBq with increased ^{177}Lu-activity.

The functional effects on the kidneys after injection with ^{177}Lu-octreotate, measured with ^{99m}Tc-DTPA scintigraphy revealed an increasing ^{99m}Tc accumulation in kidneys in the 90 or 150 MBq groups at 8 and 12 months after ^{177}Lu-octreotate injection. Furthermore the activity content in the urinary bladder seemed to decrease with increased absorbed dose and time, Figure 4.4. The 150 MBq group at 12 months could not be measured since the mice were killed due to reduced physical condition.

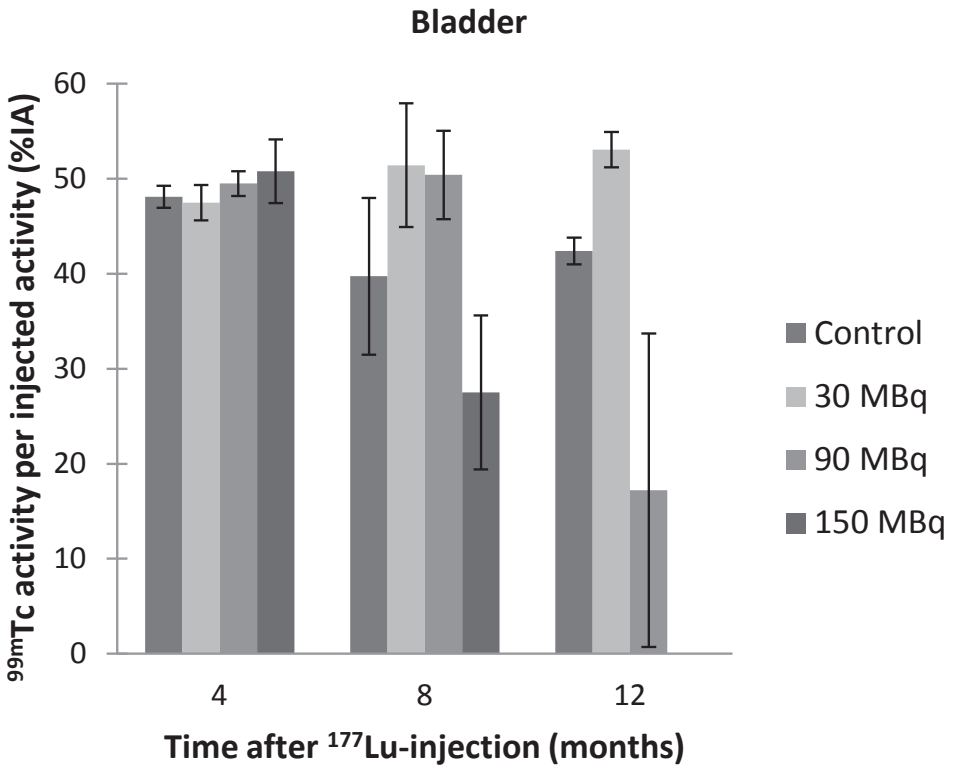

Figure 4-4 The mean bladder activity content after 27.3 min after ^{99m}Tc-DTPA administration, 4, 8 and 12 months after injection of 0-150 MBq ^{177}Lu-octreotate.

Evaluation of data from the ^{99m}Tc-DMSA scintigraphy showed a significantly increased kidney uptake compared with controls (observed at 4 months) for

the 30 and 150 MBq groups injected with ^{177}Lu-octreotate ($p<0.05$). Furthermore, an increased accumulation of ^{99m}Tc was observed at 8 and 12 months compared with that at 4 months.

Altogether the mean white blood cell count was reduced by a factor 2 for all groups compared with control, at 4 months (no more data available). The urea levels in blood at 12 months after 150 MBq ^{177}Lu administration were increased by a factor 5, while no difference was seen in the other groups at any time-point.

The gene expression analyses revealed altered regulation of some genes previously associated with radiation damage or kidney injury. Also interesting genes not previously associated with radiation damage or kidney injury had dose-dependent transcript pattern.

Paper IV

Effects of DMSA

The lowest uptake in kidneys was obtained by 1 mg of DMSA given 2 h before administration of ^{111}In-octreotide, with a mean reduction in uptake of ca 35%, (Figure 4.5). Similar effect was also obtained when 4 mg DMSA was given simultaneously or 1 h before administration of ^{111}In-octreotide. None of these differences were statistically significant. In most other organs DMSA gave no statistically significant effect on ^{111}In concentration compared to controls. Exceptions were higher ^{111}In concentration in pancreas and spleen, and lower concentration in lungs in some groups.

Effects of lysine

The lowest uptake in kidneys was obtained when 8 mg lysine was administered simultaneously with ^{111}In-octreotide, with a mean reduction in uptake of 50% ($p=0.057$), (Figure 4.5). In most other organs no statistically significant effect on ^{111}In concentration was found compared to controls. Exceptions were reduced uptake in lungs and increased uptake in pancreas, in some groups.

Effects of DMSA and lysine

The lowest uptake in kidneys was obtained when 2 mg DMSA and 8 mg lysine were given immediately before administration of ^{111}In-octreotide, Figure 4.5. This difference was not statistically different from control. Thus, no synergistic effects were obtained between DMSA and lysine. In most other organs no statistically significant effects on ^{111}In concentration was found compared to controls. Exceptions were reduced uptake in lungs, and increased uptake in blood, bone marrow, spleen and pancreas, in some groups.

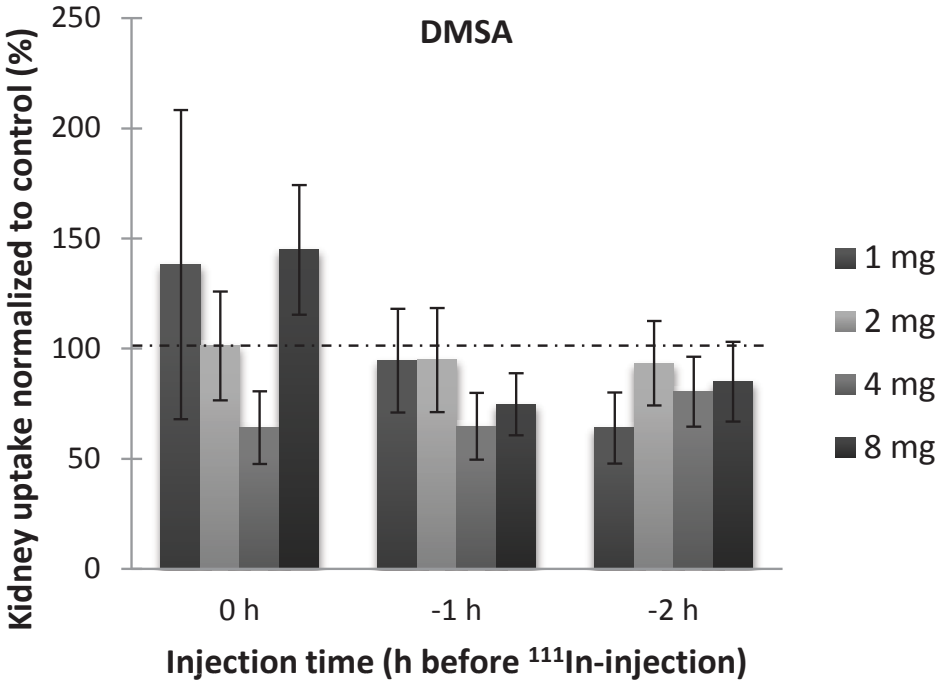

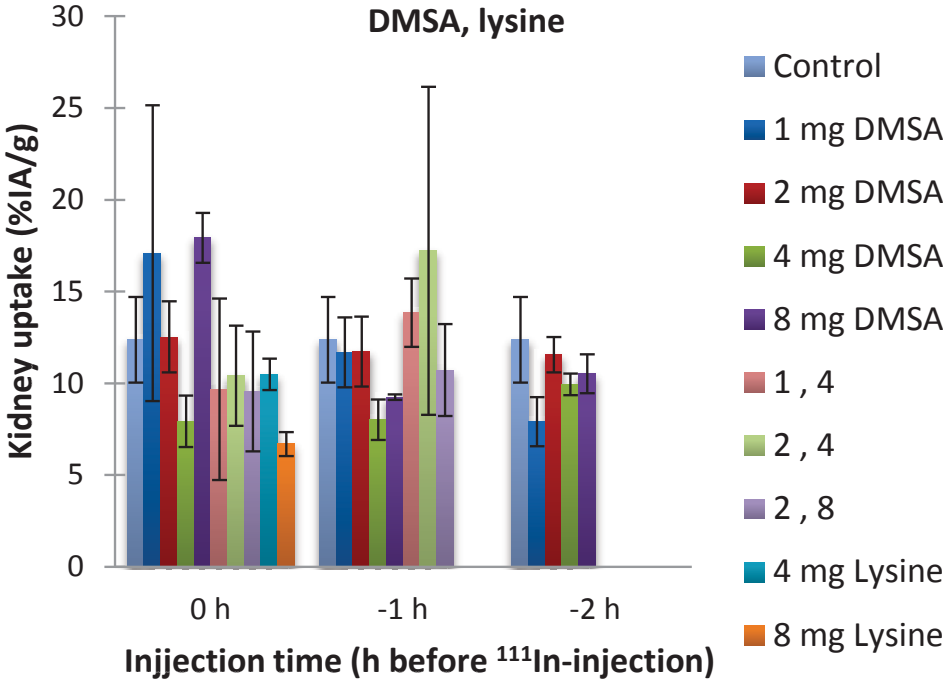

Figure 4-5 ^{111}In-octreotide uptake after i.v. injection with DMSA (1-8 mg), lysine (4 or 8 mg) or in combination (1 or 2 mg DMSA with 4 or 8 mg lysine) of both, at -2, -1 and 0 h before ^{111}In-injection.

5 DISCUSSION

PRRT with the somatostatin analog ^{177}Lu-[DOTA^0, Tyr^3]-octreotate (^{177}Lu-octreotate) has shown promising tumor effects and many patients with spread tumor disease have experienced symptomatic relief, but few patients undergo complete remission. The main limiting factor for therapy with ^{177}Lu-octreotate is toxicity of kidneys and bone marrow. The tolerance doses used are based on experience from external radiotherapy (Emami, et al., 1991, Gupta, et al., 2013, Marks, et al., 2010). Initially a cumulative (all treatment-cycles included) absorbed dose to the kidneys was set to 23 Gy, but later 28 Gy is generally applied (Bodei, et al., 2011, Bodei, et al., 2009). After infusion of ^{177}Lu-octreotate, ^{177}Lu is mainly excreted via the kidneys but also reabsorbed and accumulated in the kidneys and especially in the proximal tubular cells. However, the mechanisms behind this accumulation are not fully understood; studies indicate that some mechanisms are receptor mediated endocytosis (megalin/cubilin receptors and SSTRs), pinocytosis, ion, amino acid or oligopeptide transporters, and passive diffusion (Forssell-Aronsson, et al., 2013, Vegt, et al., 2010). Furthermore in effort to optimize ^{177}Lu-octreotate therapy, more knowledge of the biodistribution, biokinetics, and dosimetry in primarily kidney and bone marrow but also for other tissues such as liver and spleen are needed for correlation with radiobiological effects and toxicity to find relevant tolerance doses and validate new and more optimal biomarkers for toxicity. It is also of great value to estimate the absorbed dose to metastases of NET for correlation with therapeutic effects and get a better understanding of radiosensitivity of these tumors.

In the present work, $D/A_{administered}$ to kidneys was obtained from planar scintigraphic images using CV-method, curve fitting to time-activity data and MIRD formalism. Previous dosimetric studies have used various approaches. Many used planar scintigraphy and others used SPECT sometimes together with planar images. There were also different ways of how ROIs were outlined as well as location of background ROIs. Furthermore, different dosimetric methods were used with various approximations, as well as the use of different software and kidney protection agents. However, despite the method used for estimation of $D/A_{administered}$, the data from the present study were in line with those from others both regarding kidneys, liver, spleen and bone marrow (Bodei, et al., 2011, Cremonesi, et al., 2010, Cremonesi, et al., 2006, Filice, et al., 2012, Forrer, et al., 2009, Garkavij, et al., 2010, Gupta, et al., 2013, Kam, et al., 2012, Kwekkeboom, et al., 2001, Sandstrom, et al., 2013, Sandstrom, et al., 2010, Wehrmann, et al., 2007). The less labor-

consuming PA-method gave too low $D/A_{administered}$ to kidneys, and the CV method is thus preferred, at least for kidney dosimetry.

There was a large difference in $D/A_{administered}$ to kidneys and bone marrow in the present study, both between different patients and for different TCs in the same patient, with up to a factor of 8-9 in difference. A large spread among patients was also found by others (Cremonesi, et al., 2010, Cremonesi, et al., 2006, Garkavij, et al., 2010, Gupta, et al., 2013, Kwekkeboom, et al., 2001, Sandstrom, et al., 2010, Wehrmann, et al., 2007). Kidneys and bone marrow are the organs that are assumed to be critical for this treatment (Esser, et al., 2006). High $D/A_{administered}$ was also found for spleen but no toxicity related to spleen has been discussed in the litterature. Liver received in general low $D/A_{administered}$ but if metastases were included in the calculations much higher values were obtained. It might therefore be wise to study potential toxicity in patients with large tumor burden (especially many small metastases) in the liver more closely. In general the $D/A_{administered}$ to tumor decreased with each treatment cycle and the main contribution to the total absorbed dose came from the first two treatment cycles, in accordance with another study (Garkavij, et al., 2010).

Altogether, the critical organs in ^{177}Lu-octreotate treatment are bone marrow (acute and usually reversible toxicity) and kidneys (usually late toxicity, that might persist or maybe be reversible). The tolerance doses applied in ^{177}Lu-octreotate therapy today, defined as the absorbed dose where there is 5% and 50% probability of 5% organ failure in five years after treatment (TD5/5 and TD50/5) were defined for external radiation therapy (Emami, et al., 1991). Since few acute or late toxic effects have been reported TDs for ^{177}Lu-octreotate are most probably higher than for external therapy (Bodei, et al., 2011, Dorn, et al., 2003, Forrer, et al., 2009). The large differences in $D/A_{administered}$ between patients, but also between TCs for one patient, together with the limited side effects reported so far, indicate that one major way to optimize is individualized treatment planning. If tolerance doses can be determined for kidneys for ^{177}Lu-octreotate exposure, the number of fractions that can be given to a patient can be defined based on individual dosimetry for each TC. The optimal activity given per TC is not defined, and it has been suggested to reduce the activity per TC, to reduce risk for bone marrow toxicity (Bodei, et al., 2011).

If individual dosimetry based on scintigraphy should be used as a basis for individualized treatment schedule to give patients as high amount of ^{177}Lu-octreotate as possible, reliable dosimetric methods most be used. Today, planar scintigraphy and CV-methods is commonly used. This strategy has

limitations, especially when used for ^{177}Lu-octreotate. The organ delineation and determination of activity content might be difficult, together with problems in locating relevant background ROI, due to unpredictable uptake in surrounding tissues (e.g. intestines) and tumors. One way to reduce such problems can be to include SPECT examinations (Garkavij, et al., 2010).

Another simplification that affects the certainty in dosimetric estimation is the curve-fitting to the time-activity data. Mono-exponential fitting is most often used, while a multi-exponential curve would be preferable. However, then more data points (examination time-points) are needed, which might be a practical clinical limitation.

In all dosimetric estimations the accuracy of the mass of the organ is important. It would be preferable to use high quality MRI or CT images for volume determination. MIRD formalism is then most often used based on standard geometry of the organs and tissues within the body.

To estimate the absorbed dose to bone marrow, scintigraphy should be complemented with activity concentration in bone marrow biopsies (or blood samples) (Forrer, et al., 2009, Hindorf, et al., 2010).

Also the activity in sacrum could be measured and used (Siegel, et al., 1989), but the ^{177}Lu-activity in sacrum was not higher than in adjacent background, and overlapping ^{177}Lu activity in intestines and tumours in the present work made it hard to outline the sacrum area in the scintigrafic images of ^{177}Lu-octreotate.

Another way to optimize PRRT might be to identify biomarkers for radiation induced renal toxicity. In paper III functional data were compared with blood data and transcriptional data performed with RNA microarray analysis to identify biomarkers for radiation induced renal toxicity.

Altered renal function, mainly based on ^{99m}Tc-DTPA scintigraphy and blood urea level, was seen in the groups that received the highest ^{177}Lu activities at late time-points revealing clear negative effects on renal functions with increased absorbed dose to the kidneys and time after administration. No obvious functional effects were found in the low activity group, but were clearly evident in the high activity groups, and few mice from the highest activity group (150 MBq) survived up to 12 months.

A clear reduction of ^{99m}Tc-DTPA excretion into the bladder for was seen for highest activities and at late time-points, while no effects on renal clearance

of ^{99m}Tc could be observed for lowest activity at any time point studied. The bladder ^{99m}Tc-activity content was lower for the groups with altered clearance curves. To our knowledge no study has demonstrated such effects after irradiation with ^{177}Lu-octreotate. Instead, the uptake of ^{111}In-DTPA in kidneys was reduced in rats after treatment with ^{177}Lu-octreotate (Melis, et al., 2010). Reduced excretion has previously been demonstrated in calculi in the kidney pelvis or ureters, i.e. nephrolithiasis (Hecht, et al., 2010).

Furthermore, no reduction in renal uptake of ^{99m}Tc-DMSA was seen, only increased uptake at 4 months, a finding difficult to explain. Previous studies on rats revealed clear reduction in kidney uptake of ^{99m}Tc-DMSA after ^{177}Lu-octreotate treatment (Forrer, et al., 2007, Melis, et al., 2010). However, an altered renal function, as demonstrated by the ^{99m}Tc-DTPA renogram, might hide an otherwise reduced uptake.

The histological evaluation revealed glomerular segmentalization and signs of nodular sclerosis for the two highest activities at 8 and 12 months, with prominent nucleolar and nuclear fragmentation observed as well as focal and segmental necrosis. Another histological study on rats showed that low ^{177}Lu-activities gave mainly proximal tubular damage, while high amounts of ^{177}Lu caused damage of the distal tubules (Forrer, et al., 2007). In a study on nude mice, toxicity was also found mainly in proximal tubules (Svensson, et al., 2012).

Altogether, the study indicates that the tolerance dose for kidneys in normal mice injected with ^{177}Lu-octreotate can be found in the range 19-45 Gy after a single injection. In a similar study on nude mice a threshold absorbed dose for toxicity was defined at 24 Gy (Svensson, et al., 2012), and that level is most probably higher in normal mice with complete immune system. It is not possible to directly translate these data to humans, due to e.g. different sizes of kidney in relation to the range of electrons emitted and different uptake mechanisms (expression of receptors and transporters differ between species). The microarray data indicate interesting radiation-related genes that might be useful when defining new biomarkers for late kidney toxicity.

The kidney handling of ^{177}Lu-octreotate and ^{111}In-octreotide are not fully known, but proximal tubule cells are believed to be of great importance for the uptake (Rolleman, et al., 2010). As previously described the reabsorption is probably mediated by several transport mechanisms, e.g. via SSTR and megalin/cubilin receptors, amino acid/oligopeptide transporters, passive diffusion and pinocytosis (Forssell-Aronsson, et al., 2013, Vegt, et al., 2010). Since the kidney blocking effect by the agents used today in patients (e.g.

lysine and arginine) is limited there is a need to find more efficient blocking strategies and increased knowledge of the retention mechanisms in kidneys.

A combination of lysine and DMSA could be one option, since they seem to interact by different mechanisms, both tubular reabsorption and tubular secretion and reabsorption. However, we did not find a synergistic effect using lysine and DMSA together, rather the opposite, with a higher activity concentration in kidneys. One reason for these unwanted results could be that the time between the administrations is important and that DMSA should be given after administration of the radiopharmaceutical, as demonstrated for ^{177}Lu-octreotate in rats (Moorin, et al., 2007). Another reason could be that both lysine and DMSA are reabsorbed by the megalin/cubilin-mediated endocytosis as recently presented by Weyer et al. (Weyer, et al., 2013).

There were no clear trend of reduced or increased uptake of ^{111}In-octreotide in most tissue other than kidneys (i.e. bone marrow, blood, liver, spleen and pancreas), in accordance with previously presented data on ^{177}Lu-octreotate in rats (Moorin, et al., 2007), although lower uptake was found in lungs and pancreas, and higher concentration in bone marrow, blood and spleen for some of the groups. Further work is needed for better understanding of the effects of lysine and DMSA on biokinetics of radiolabeled SS analogues, both in kidneys and other tissues. Optimization of amounts and time between administrations should be done. Furthermore, other agents should be studied in a similar way to enhance blocking of kidney uptake without higher concentration in bone marrow and blood.

6 CONCLUSION

The pharmacokinetics of ^{177}Lu-octreotate in patients with NETs was determined using planar scintigraphy. Large individual differences in time-activity curves were obtained for kidneys, liver and spleen, while the relative whole body activity content and retention time followed the same curve form. In general the time activity curves for kidney and spleen had similar curve form, with an uptake phase followed by a slow excretion, while the liver had a much faster uptake phase (shorter than 1 h) and only excretion was demonstrated. The ^{177}Lu uptake in tumors had an uptake phase during the first days after injection followed by a slow excretion. The activity uptake in tumors became lower with each treatment cycle, probably due to treatment effects.

The absorbed dose per administered activity was determined for kidneys, liver, spleen, red marrow and tumor tissue in patients with NET treated with ^{177}Lu-octreotate. Large variations were found for each normal tissue type between patients and between administrations in the same patient, clearly demonstrating the importance of individualized dosimetric calculations when using ^{177}Lu-octreotate for therapy. High absorbed dose was found in many metastases.

The radiobiological effects on kidneys investigated in normal mice revealed negative effects on renal function, which was enhanced with increased absorbed dose to kidneys and elapsed time after ^{177}Lu-octreotate injection, mainly based on ^{99m}Tc-DTPA scintigraphy and blood urea level. The observed transcriptional response revealed several radiation responding genes, e.g. *Cdkn1a*, *Dbp*, and *Per2,* that could be useful when suggesting potential biomarkers for early prediction of late renal toxicity and impairment.

Lysine is today used as kidney blocker of ^{177}Lu-octreotate. DMSA given alone gave similar blocking effects as lysine of the uptake of ^{111}In-octreotide in kidneys, a reduction of 35-45%. However, no additive effects were obtained when DMSA and lysine were combined. The reason is probably a non-optimal time schedule between administrations. Higher blocking effects of DMSA would probably be seen if DMSA was given after ^{111}In-octreotide.

7 FUTURE PERSPECTIVES

This work clearly shows some options for optimization of therapy using ^{177}Lu-octreotate. To continue and develop more optimized treatment, much work remains to be done.

The tolerance doses applied in ^{177}Lu-octreotate therapy today are those defined for external radiation therapy. Since few acute or late toxic effects have been reported, TDs for ^{177}Lu-octreotate are most probably much higher than for external therapy. Thus, thoroughly designed clinical studies should be performed where physiological parameters are followed, including acute and late renal effects.

Furthermore, standardized methods for absolute activity quantification and dosimetry based on scintigraphy should be defined and used by all clinics, to ensure high quality of data and enable comparison between centers and studies. Such standards should include acquisition methods (SPECT and planar scintigraphy, choice of energy window and collimator, and time-points for imaging, especially late time-points), calibration (using suitable phantoms), attenuation and scatter correction, image analysis including delineation of the organ and background ROI, the use of CT and MR images for organ delineation etc. Such methods would enhance future ability to define tolerance dose values for this treatment modality, and enable more patient-specific therapy.

The radiobiological effects on kidneys must be studied more extensively both in animals and patients in order to understand the mechanisms involved in kidney toxicity. Based on such knowledge it would be easier to develop suitable biomarkers for kidney toxicity. The biomarkers used today, e.g. parameters based on scintigraphy using ^{99m}Tc-labeled DTPA, DMSA and MAG3 should be investigated together with biomarker levels in easily available body fluids such as blood and urine and correlated with absorbed dose to kidneys and clinically observed kidney toxicity. Based on such studies relevant tolerance doses to kidneys from irradiation with ^{177}Lu-octreotate could be defined. New biomarkers might be suggested based on results from microarray analysis of kidney tissue after irradiation.

Kidney blocking of ^{177}Lu-octreotate should be further studied and optimized. More knowledge on how the kidney handles DMSA, lysine and ^{177}Lu-octreotate is clearly needed. Both dosage and timing must be studied and

optimized. Also the usefulness and toxicity of other kidney blocking agents should be examined.

It has also been proposed that biological effective dose (BED) should be discussed and use in radionuclide therapy. This requires better knowledge of biological factors of the tumor tissue, such as repair, radiosensitivity, repopulation and evaluation of the LQ model for NETs and ^{177}Lu-octreotate. Such data should be collected in well-designed clinical studies and is needed to better understand and hopefully optimize the therapeutic effects on tumor tissue.

ACKNOWLEDGEMENT

I would like to express my gratitude to my research supervisor Eva Forssell-Aronsson, for her patient guidance, enthusiastic encouragement and useful critiques of this research work, and to my co-supervisor Peter Bernhardt, for introducing me to this research field.

My specials thanks to Kecke Elmroth, for her advice and support and for keeping me stay in progress. I deeply want to express my appreciation to Anders for his valuable and constructive help during the writing and development of this research work, and to Johanna for her happiness and for always telling me that this is fun. Moreover, I would like to express my gratitude to Linda, Tara, Emilia and Elin, who never failed to listen and support me. I would also like to extend my thanks to Lars Jacobsson– your advice has been of great help. Other special thanks to Nils, Johan, Micke, Britta, Emil, Esmaeil, Ingun and Viktor for being a great fun group to belong to, and to Mia for always making me laugh whenever needed. To Jenny, Angelika, Janette, Helena, Alexa, Tom, Anna, Lotta, Niklas, Magnus, Caroline and Sofia, thanks for all the fun at "fika" and lunch times. And to all you guys that are in my heart–but not in my head–at this moment when writing.

I am particularly grateful for the skilled technical assistance given by Lilian and Ann, and to Gunilla for always helping. To Agnetha Gustafsson and Jakobína Grétarsdóttir for introducing me to nuclear medicine, and for the help from colleagues at Medical Physics and Medical Bioengineering and Centrala Isotopintaget at Sahlgrenska; Jacob and The Ladies at Nuclear Medicine for letting me draw my ROIs, Barbro and Petra for always being so helpful.

Thanks to my co-authors: Håkan Ahlman, Bo Wängberg, Gertrud Berg, Johanna Svensson, Khalil Helou, Toshima Parris, Martin Johansson and Andreas Österlund.

Finally, I wish to thank my parents Elvy and Lars-Erik and my sisters Therese and Linnéa for their everlasting support and encouragement throughout life. And I sincerely need to praise my family: thank you Denise for being so loving and caring, Jasmine for always being so close to laughter and joy and Nellie for keeping me sane and teaching me how to love and what's important in life. I would be nothing without you!

And to my beloved husband **Hans**, words cannot say what your love and support means to me. **I will love you always**.

This work was supported by grants from the Swedish Research Council (grant no. 21073), the Swedish Cancer Society (grant no. 3427), BioCARE - a National Strategic Research Program at the University of Gothenburg, the Swedish Radiation Safety Authority, the King Gustav V Jubilee Clinic Cancer Research Foundation, the Sahlgrenska University Hospital Research Funds, the Assar Gabrielsson Cancer Research Foundation, the Lions Cancerfond Väst, the Adlerbertska Research Foundation, the Lars Hierta Memorial Foundation, the the Royal Society of Arts and Sciences in Gothenburg (KVVS). Parts of the work was performed within the EC COST Action BM0607.

REFERENCES

Ahlman H, Tisell LE, Wangberg B, Nilsson O, Forssell-Aronsson E, Fjalling M: **Somatostatin receptor imaging in patients with neuroendocrine tumors: preoperative and postoperative scintigraphy and intraoperative use of a scintillation detector**. *Seminars in oncology* 1994, **21**(5 Suppl 13):21-28.

Andersson P, Forssell-Aronsson E, Johanson V, Wangberg B, Nilsson O, Fjalling M, Ahlman H: **Internalization of indium-111 into human neuroendocrine tumor cells after incubation with indium-111-DTPA-D-Phe1-octreotide**. *Journal of nuclear medicine : official publication, Society of Nuclear Medicine* 1996, **37**(12):2002-2006.

Bagshaw SM, Bellomo R: **Cystatin C in acute kidney injury**. *Current opinion in critical care* 2010, **16**(6):533-539.

Barbieri F, Bajetto A, Pattarozzi A, Gatti M, Wurth R, Thellung S, Corsaro A, Villa V, Nizzari M, Florio T: **Peptide receptor targeting in cancer: the somatostatin paradigm**. *International journal of peptides* 2013, **2013**:926295.

Bernard BF, Krenning EP, Breeman WA, Rolleman EJ, Bakker WH, Visser TJ, Macke H, de Jong M: **D-lysine reduction of indium-111 octreotide and yttrium-90 octreotide renal uptake**. *Journal of nuclear medicine : official publication, Society of Nuclear Medicine* 1997, **38**(12):1929-1933.

Bodei L, Cremonesi M, Grana CM, Fazio N, Iodice S, Baio SM, Bartolomei M, Lombardo D, Ferrari ME, Sansovini M *et al*: **Peptide receptor radionuclide therapy with (1)(7)(7)Lu-DOTATATE: the IEO phase I-II study**. *European journal of nuclear medicine and molecular imaging* 2011, **38**(12):2125-2135.

Bodei L, Ferone D, Grana CM, Cremonesi M, Signore A, Dierckx RA, Paganelli G: **Peptide receptor therapies in neuroendocrine tumors**. *Journal of endocrinological investigation* 2009, **32**(4):360-369.

Bolch WE, Eckerman KF, Sgouros G, Thomas SR: **MIRD pamphlet No. 21: a generalized schema for radiopharmaceutical dosimetry--standardization of nomenclature**. *Journal of nuclear medicine : official publication, Society of Nuclear Medicine* 2009, **50**(3):477-484.

Bousquet C, Lasfargues C, Chalabi M, Billah SM, Susini C, Vezzosi D, Caron P, Pyronnet S: **Clinical review: Current scientific rationale for the use of somatostatin analogs and mTOR inhibitors in neuroendocrine tumor therapy**. *The Journal of clinical endocrinology and metabolism* 2012, **97**(3):727-737.

Buijs WC, Siegel JA, Boerman OC, Corstens FH: **Absolute organ activity estimated by five different methods of background correction**.

Journal of nuclear medicine : official publication, Society of Nuclear Medicine 1998, **39**(12):2167-2172.

Capello A, Krenning EP, Breeman WA, Bernard BF, de Jong M: **Peptide receptor radionuclide therapy in vitro using [111In-DTPA0]octreotide**. *Journal of nuclear medicine : official publication, Society of Nuclear Medicine* 2003, **44**(1):98-104.

Carbonnel C, Seux V, Pauly V, Oddoze C, Roubicek C, Larue JR, Thirion X, Soubeyrand J, Retornaz F: **[Estimation of the glomerular filtration rate in elderly inpatients: comparison of four methods]**. *La Revue de medecine interne / fondee par la Societe nationale francaise de medecine interne* 2008, **29**(5):364-369.

Carlsson J, Forssell-Aronsson E, Glimelius B, Mattsson S, Swedish Cancer Society Investigation G: **Therapy with radiopharmaceuticals**. *Acta oncologica* 2002, **41**(7-8):623-628.

Carlsson J, Forssell Aronsson E, Hietala SO, Stigbrand T, Tennvall J: **Tumour therapy with radionuclides: assessment of progress and problems**. *Radiotherapy and oncology : journal of the European Society for Therapeutic Radiology and Oncology* 2003, **66**(2):107-117.

Cherry SR, Sorenson JA, Phelps ME: **Physics in nuclear medicine**, 4th edn. Philadelphia: Elsevier/Saunders; 2012.

Christensen EI, Birn H: **Megalin and cubilin: synergistic endocytic receptors in renal proximal tubule**. *American journal of physiology Renal physiology* 2001, **280**(4):F562-573.

Christensen EI, Birn H: **Megalin and cubilin: multifunctional endocytic receptors**. *Nature reviews Molecular cell biology* 2002, **3**(4):256-266.

Christensen EI, Birn H, Verroust P, Moestrup SK: **Megalin-mediated endocytosis in renal proximal tubule**. *Renal failure* 1998, **20**(2):191-199.

Christensen EI, Verroust PJ, Nielsen R: **Receptor-mediated endocytosis in renal proximal tubule**. *Pflugers Archiv : European journal of physiology* 2009, **458**(6):1039-1048.

Cohen EP, Moulder JE, Robbins ME: **Radiation nephropathy caused by yttrium 90**. *Lancet* 2001, **358**(9287):1102-1103.

Cremonesi M, Botta F, Di Dia A, Ferrari M, Bodei L, De Cicco C, Rossi A, Bartolomei M, Mei R, Severi S *et al*: **Dosimetry for treatment with radiolabelled somatostatin analogues. A review**. *The quarterly journal of nuclear medicine and molecular imaging : official publication of the Italian Association of Nuclear Medicine* 2010, **54**(1):37-51.

Cremonesi M, Ferrari ME, Bodei L, Bartolomei M, Chinol M, Mei R, Daou B, Tosi G, Paganelli G: **Dosimetry in patients undergoing Lu-177-DOTATATE therapy with indications for Y-90-DOTATATE**.

European journal of nuclear medicine and molecular imaging 2006, **33**:S102-S102.

Csaba Z, Dournaud P: **Cellular biology of somatostatin receptors**. *Neuropeptides* 2001, **35**(1):1-23.

Daniel GB, Mitchell SK, Mawby D, Sackman JE, Schmidt D: **Renal nuclear medicine: a review**. *Veterinary radiology & ultrasound : the official journal of the American College of Veterinary Radiology and the International Veterinary Radiology Association* 1999, **40**(6):572-587.

de Jong M, Barone R, Krenning E, Bernard B, Melis M, Visser T, Gekle M, Willnow TE, Walrand S, Jamar F *et al*: **Megalin is essential for renal proximal tubule reabsorption of (111)In-DTPA-octreotide**. *Journal of nuclear medicine : official publication, Society of Nuclear Medicine* 2005, **46**(10):1696-1700.

de Lange MJ, Piers DA, Kosterink JG, van Luijk WH, Meijer S, de Zeeuw D, van der Hem GK: **Renal handling of technetium-99m DMSA: evidence for glomerular filtration and peritubular uptake**. *Journal of nuclear medicine : official publication, Society of Nuclear Medicine* 1989, **30**(7):1219-1223.

Dorn R, Kopp J, Vogt H, Heidenreich P, Carroll RG, Gulec SA: **Dosimetry-guided radioactive iodine treatment in patients with metastatic differentiated thyroid cancer: largest safe dose using a risk-adapted approach**. *Journal of nuclear medicine : official publication, Society of Nuclear Medicine* 2003, **44**(3):451-456.

Emami B, Lyman J, Brown A, Coia L, Goitein M, Munzenrider JE, Shank B, Solin LJ, Wesson M: **Tolerance of normal tissue to therapeutic irradiation**. *Int J Radiat Oncol Biol Phys* 1991, **21**(1):109-122.

Emami B, Lyman J, Brown A, Coia L, Goitein M, Munzenrider JE, Shank B, Solin LJ, Wesson M: **Tolerance of normal tissue to therapeutic irradiation**. *International journal of radiation oncology, biology, physics* 1991, **21**(1):109-122.

Esser JP, Krenning EP, Teunissen JJ, Kooij PP, van Gameren AL, Bakker WH, Kwekkeboom DJ: **Comparison of [(177)Lu-DOTA(0),Tyr(3)]octreotate and [(177)Lu-DOTA(0),Tyr(3)]octreotide: which peptide is preferable for PRRT?** *European journal of nuclear medicine and molecular imaging* 2006, **33**(11):1346-1351.

Fenton RA, Knepper MA: **Urea and renal function in the 21st century: insights from knockout mice**. *Journal of the American Society of Nephrology : JASN* 2007, **18**(3):679-688.

Ferjoux G, Bousquet C, Cordelier P, Benali N, Lopez F, Rochaix P, Buscail L, Susini C: **Signal transduction of somatostatin receptors negatively controlling cell proliferation**. *Journal of physiology, Paris* 2000, **94**(3-4):205-210.

Filice A, Fraternali A, Frasoldati A, Asti M, Grassi E, Massi L, Sollini M, Froio A, Erba PA, Versari A: **Radiolabeled somatostatin analogues**

therapy in advanced neuroendocrine tumors: a single centre experience. *Journal of oncology* 2012, **2012**:320198.

Fjalling M, Andersson P, Forssell-Aronsson E, Gretarsdottir J, Johansson V, Tisell LE, Wangberg B, Nilsson O, Berg G, Michanek A *et al*: **Systemic radionuclide therapy using indium-111-DTPA-D-Phe1-octreotide in midgut carcinoid syndrome**. *Journal of nuclear medicine : official publication, Society of Nuclear Medicine* 1996, **37**(9):1519-1521.

Fleming JS: **A technique for the absolute measurement of activity using a gamma camera and computer**. *Phys Med Biol* 1979, **24**(1):176-180.

Forrer F, Krenning EP, Kooij PP, Bernard BF, Konijnenberg M, Bakker WH, Teunissen JJ, de Jong M, van Lom K, de Herder WW *et al*: **Bone marrow dosimetry in peptide receptor radionuclide therapy with [177Lu-DOTA(0),Tyr(3)]octreotate**. *European journal of nuclear medicine and molecular imaging* 2009, **36**(7):1138-1146.

Forrer F, Rolleman E, Bijster M, Melis M, Bernard B, Krenning EP, de Jong M: **From outside to inside? Dose-dependent renal tubular damage after high-dose peptide receptor radionuclide therapy in rats measured with in vivo (99m)Tc-DMSA-SPECT and molecular imaging**. *Cancer biotherapy & radiopharmaceuticals* 2007, **22**(1):40-49.

Forssell-Aronsson E, Bernhardt P, Nilsson O, Tisell LE, Wangberg B, Ahlman H: **Biodistribution data from 100 patients i.v. injected with 111In-DTPA-D-Phe1-octreotide**. *Acta oncologica* 2004, **43**(5):436-442.

Forssell-Aronsson E, Spetz J, Ahlman H: **Radionuclide therapy via SSTR: future aspects from experimental animal studies**. *Neuroendocrinology* 2013, **97**(1):86-98.

Freitas RS, Gutfilen B, da Fonseca LM, Bernardo-Filho M: **Evaluation of 99mtechnetium-radiopharmaceutical binding to blood elements using different trichloroacetic acid concentrations**. *The Yale journal of biology and medicine* 1996, **69**(6):483-488.

Garkavij M, Nickel M, Sjogreen-Gleisner K, Ljungberg M, Ohlsson T, Wingardh K, Strand SE, Tennvall J: **177Lu-[DOTA0,Tyr3] octreotate therapy in patients with disseminated neuroendocrine tumors: Analysis of dosimetry with impact on future therapeutic strategy**. *Cancer* 2010, **116**(4 Suppl):1084-1092.

Grozinsky-Glasberg S, Grossman AB, Korbonits M: **The role of somatostatin analogues in the treatment of neuroendocrine tumours**. *Molecular and cellular endocrinology* 2008, **286**(1-2):238-250.

Grozinsky-Glasberg S, Shimon I, Korbonits M, Grossman AB: **Somatostatin analogues in the control of neuroendocrine tumours: efficacy and mechanisms**. *Endocrine-related cancer* 2008, **15**(3):701-720.

Guillermet-Guibert J, Lahlou H, Cordelier P, Bousquet C, Pyronnet S, Susini C: **Physiology of somatostatin receptors**. *Journal of endocrinological investigation* 2005, **28**(11 Suppl International):5-9.

Guillermet-Guibert J, Lahlou H, Pyronnet S, Bousquet C, Susini C: **Somatostatin receptors as tools for diagnosis and therapy: Molecular aspects**. *Best Practice & Research Clinical Gastroenterology* 2005, **19**(4):535-551.

Gupta SK, Singla S, Thakral P, Bal CS: **Dosimetric analyses of kidneys, liver, spleen, pituitary gland, and neuroendocrine tumors of patients treated with 177Lu-DOTATATE**. *Clinical nuclear medicine* 2013, **38**(3):188-194.

Gustafsson BI, Kidd M, Modlin IM: **Neuroendocrine tumors of the diffuse neuroendocrine system**. *Current opinion in oncology* 2008, **20**(1):1-12.

Hall EJ, Giaccia AJ: **Radiobiology for the radiologist**, 6th edn. Philadelphia: Lippincott Williams & Wilkins; 2006.

Haraldsson B: **Tubular reabsorption of albumin: it's all about cubilin**. *Journal of the American Society of Nephrology : JASN* 2010, **21**(11):1810-1812.

Haraldsson B, Nystrom J, Deen WM: **Properties of the glomerular barrier and mechanisms of proteinuria**. *Physiological reviews* 2008, **88**(2):451-487.

Hecht S, Lawson SM, Lane IF, Sharp DE, Daniel GB: **(99m)Tc-DTPA diuretic renal scintigraphy in dogs with nephroureterolithiasis**. *The Canadian veterinary journal La revue veterinaire canadienne* 2010, **51**(12):1360-1366.

Hindorf C, Glatting G, Chiesa C, Linden O, Flux G: **EANM Dosimetry Committee guidelines for bone marrow and whole-body dosimetry**. *European journal of nuclear medicine and molecular imaging* 2010, **37**(6):1238-1250.

Hindorf C, Glatting G, Chiesa C, Linden O, Flux G, Committee ED: **EANM Dosimetry Committee guidelines for bone marrow and whole-body dosimetry**. *European journal of nuclear medicine and molecular imaging* 2010, **37**(6):1238-1250.

ICRP38: **Radionuclide Transformations - Energy and Intensity of Emissions**. *ICRP Publication 38 Ann ICRP* 1983, **11-13**(Part 2):738-761.

ICRP107: **Nuclear Decay Data for Dosimetric Calculations**. *ICRP Publication 107* 2008, **38**(3):1-96.

Kam BL, Teunissen JJ, Krenning EP, de Herder WW, Khan S, van Vliet EI, Kwekkeboom DJ: **Lutetium-labelled peptides for therapy of neuroendocrine tumours**. *European journal of nuclear medicine and molecular imaging* 2012, **39 Suppl 1**:S103-112.

Klimstra DS: **Pathology reporting of neuroendocrine tumors: essential elements for accurate diagnosis, classification, and staging**. *Seminars in oncology* 2013, **40**(1):23-36.

Klimstra DS, Modlin IR, Coppola D, Lloyd RV, Suster S: **The pathologic classification of neuroendocrine tumors: a review of nomenclature, grading, and staging systems**. *Pancreas* 2010, **39**(6):707-712.

Krenning EP, Bakker WH, Breeman WA, Koper JW, Kooij PP, Ausema L, Lameris JS, Reubi JC, Lamberts SW: **Localisation of endocrine-related tumours with radioiodinated analogue of somatostatin**. *Lancet* 1989, **1**(8632):242-244.

Krenning EP, Bakker WH, Kooij PP, Breeman WA, Oei HY, de Jong M, Reubi JC, Visser TJ, Bruns C, Kwekkeboom DJ *et al*: **Somatostatin receptor scintigraphy with indium-111-DTPA-D-Phe-1-octreotide in man: metabolism, dosimetry and comparison with iodine-123-Tyr-3-octreotide**. *Journal of nuclear medicine : official publication, Society of Nuclear Medicine* 1992, **33**(5):652-658.

Krenning EP, de Jong M, Kooij PP, Breeman WA, Bakker WH, de Herder WW, van Eijck CH, Kwekkeboom DJ, Jamar F, Pauwels S *et al*: **Radiolabelled somatostatin analogue(s) for peptide receptor scintigraphy and radionuclide therapy**. *Annals of oncology : official journal of the European Society for Medical Oncology / ESMO* 1999, **10 Suppl 2**:S23-29.

Krutzen E, Back SE, Nilsson-Ehle I, Nilsson-Ehle P: **Plasma clearance of a new contrast agent, iohexol: a method for the assessment of glomerular filtration rate**. *The Journal of laboratory and clinical medicine* 1984, **104**(6):955-961.

Kwekkeboom DJ, Bakker WH, Kooij PP, Konijnenberg MW, Srinivasan A, Erion JL, Schmidt MA, Bugaj JL, de Jong M, Krenning EP: **[177Lu-DOTAOTyr3]octreotate: comparison with [111In-DTPAo]octreotide in patients**. *European journal of nuclear medicine* 2001, **28**(9):1319-1325.

Kwekkeboom DJ, Kam BL, van Essen M, Teunissen JJ, van Eijck CH, Valkema R, de Jong M, de Herder WW, Krenning EP: **Somatostatin-receptor-based imaging and therapy of gastroenteropancreatic neuroendocrine tumors**. *Endocrine-related cancer* 2010, **17**(1):R53-73.

Kwekkeboom DJ, Teunissen JJ, Bakker WH, Kooij PP, de Herder WW, Feelders RA, van Eijck CH, Esser JP, Kam BL, Krenning EP: **Radiolabeled somatostatin analog [177Lu-DOTA0,Tyr3]octreotate in patients with endocrine gastroenteropancreatic tumors**. *Journal of clinical oncology : official journal of the American Society of Clinical Oncology* 2005, **23**(12):2754-2762.

Lamb EJ, Stevens PE: **Estimating and measuring glomerular filtration rate: methods of measurement and markers for estimation**. *Current opinion in nephrology and hypertension* 2014, **23**(3):258-266.

Larsson M, Bernhardt P, Svensson J, Wangberg B, Ahlman H, Forssell-Aronsson E: **Estimation of absorbed dose to the kidneys in patients after treatment with 177Lu-octreotate: comparison between methods based on planar scintigraphy**. *EJNMMI research* 2012, **2**(1):49.

Lassmann M, Chiesa C, Flux G, Bardies M, Committee ED: **EANM Dosimetry Committee guidance document: good practice of clinical dosimetry reporting**. *European journal of nuclear medicine and molecular imaging* 2011, **38**(1):192-200.

Loevinger R, Budinger TF, Watson EE, Society of Nuclear Medicine (1953-). Medical Internal Radiation Dose Committee.: **MIRD primer for absorbed dose calculations**. New York, NY: Society of Nuclear Medicine; 1988.

Luxton RW: **Radiation nephritis. A long-term study of 54 patients**. *Lancet* 1961, **2**(7214):1221-1224.

Marks LB, Yorke ED, Jackson A, Ten Haken RK, Constine LS, Eisbruch A, Bentzen SM, Nam J, Deasy JO: **Use of Normal Tissue Complication Probability Models in the Clinic**. *Int J Radiat Oncol* 2010, **76**(3):S10-S19.

Melis M, de Swart J, de Visser M, Berndsen SC, Koelewijn S, Valkema R, Boerman OC, Krenning EP, de Jong M: **Dynamic and static small-animal SPECT in rats for monitoring renal function after 177Lu-labeled Tyr3-octreotate radionuclide therapy**. *Journal of nuclear medicine : official publication, Society of Nuclear Medicine* 2010, **51**(12):1962-1968.

Melis M, Krenning EP, Bernard BF, Barone R, Visser TJ, de Jong M: **Localisation and mechanism of renal retention of radiolabelled somatostatin analogues**. *European journal of nuclear medicine and molecular imaging* 2005, **32**(10):1136-1143.

Melis M, Krenning EP, Bernard BF, de Visser M, Rolleman E, de Jong M: **Renal uptake and retention of radiolabeled somatostatin, bombesin, neurotensin, minigastrin and CCK analogues: species and gender differences**. *Nuclear medicine and biology* 2007, **34**(6):633-641.

Miller WH, Hartmann-Siantar C, Fisher D, Descalle MA, Daly T, Lehmann J, Lewis MR, Hoffman T, Smith J, Situ PD *et al*: **Evaluation of beta-absorbed fractions in a mouse model for 90Y, 188Re, 166Ho, 149Pm, 64Cu, and 177Lu radionuclides**. *Cancer biotherapy & radiopharmaceuticals* 2005, **20**(4):436-449.

Moorin RE, Meyrick DP, Rose A: **Pre-clinical evaluation of 2,3-dimercaptosuccinic acid as a radiation nephrotoxicity protective**

agent during radiopeptide therapy of neuroendocrine malignancy. *Nuclear medicine communications* 2007, **28**(4):261-266.

Morel G: **Internalization and nuclear localization of peptide hormones**. *Biochemical pharmacology* 1994, **47**(1):63-76.

Norrgren K, Svegborn SL, Areberg J, Mattsson S: **Accuracy of the quantification of organ activity from planar gamma camera images**. *Cancer biotherapy & radiopharmaceuticals* 2003, **18**(1):125-131.

Osman AO, Elmadani AE: **Comparison of slope-intercept with single plasma sample methods in estimating glomerular filtration rate using radionuclides**. *Saudi journal of kidney diseases and transplantation : an official publication of the Saudi Center for Organ Transplantation, Saudi Arabia* 2014, **25**(2):321-325.

Otte A, Herrmann R, Heppeler A, Behe M, Jermann E, Powell P, Maecke HR, Muller J: **Yttrium-90 DOTATOC: first clinical results**. *European journal of nuclear medicine* 1999, **26**(11):1439-1447.

Paganelli G, Zoboli S, Cremonesi M, Macke HR, Chinol M: **Receptor-mediated radionuclide therapy with 90Y-DOTA-D-Phe1-Tyr3-Octreotide: preliminary report in cancer patients**. *Cancer biotherapy & radiopharmaceuticals* 1999, **14**(6):477-483.

Peters AM, Jones DH, Evans K, Gordon I: **Two routes for 99mTc-DMSA uptake into the renal cortical tubular cell**. *European journal of nuclear medicine* 1988, **14**(11):555-561.

Reubi JC: **Regulatory peptide receptors as molecular targets for cancer diagnosis and therapy**. *The quarterly journal of nuclear medicine : official publication of the Italian Association of Nuclear Medicine* 1997, **41**(2):63-70.

Reubi JC, Hacki WH, Lamberts SW: **Hormone-producing gastrointestinal tumors contain a high density of somatostatin receptors**. *The Journal of clinical endocrinology and metabolism* 1987, **65**(6):1127-1134.

Rolleman EJ, Bernard BF, Breeman WA, Forrer F, de Blois E, Hoppin J, Gotthardt M, Boerman OC, Krenning EP, de Jong M: **Molecular imaging of reduced renal uptake of radiolabelled [DOTA0,Tyr3]octreotate by the combination of lysine and Gelofusine in rats**. *Nuklearmedizin Nuclear medicine* 2008, **47**(3):110-115.

Rolleman EJ, Kooij PPM, de Herder WW, Valkema R, Krenning EP, de Jong M: **Somatostatin receptor subtype 2-mediated uptake of radiolabelled somatostatin analogues in the human kidney**. *European journal of nuclear medicine and molecular imaging* 2007, **34**(11):1854-1860.

Rolleman EJ, Melis M, Valkema R, Boerman OC, Krenning EP, de Jong M: **Kidney protection during peptide receptor radionuclide therapy**

with somatostatin analogues. *European journal of nuclear medicine and molecular imaging* 2010, **37**(5):1018-1031.

Rolleman EJ, Valkema R, de Jong M, Kooij PP, Krenning EP: **Safe and effective inhibition of renal uptake of radiolabelled octreotide by a combination of lysine and arginine**. *European journal of nuclear medicine and molecular imaging* 2003, **30**(1):9-15.

Sandstrom M, Garske-Roman U, Granberg D, Johansson S, Widstrom C, Eriksson B, Sundin A, Lundqvist H, Lubberink M: **Individualized dosimetry of kidney and bone marrow in patients undergoing 177Lu-DOTA-octreotate treatment**. *Journal of nuclear medicine : official publication, Society of Nuclear Medicine* 2013, **54**(1):33-41.

Sandstrom M, Garske U, Granberg D, Sundin A, Lundqvist H: **Individualized dosimetry in patients undergoing therapy with (177)Lu-DOTA-D-Phe (1)-Tyr (3)-octreotate**. *European journal of nuclear medicine and molecular imaging* 2010, **37**(2):212-225.

Schneider CA, Rasband WS, Eliceiri KW: **NIH Image to ImageJ: 25 years of image analysis**. *Nature methods* 2012, **9**(7):671-675.

Siegel JA, Lee RE, Pawlyk DA, Horowitz JA, Sharkey RM, Goldenberg DM: **Sacral scintigraphy for bone marrow dosimetry in radioimmunotherapy**. *International journal of radiation applications and instrumentation Part B, Nuclear medicine and biology* 1989, **16**(6):553-559.

Siegel JA, Stabin MG: **Absorbed fractions for electrons and beta particles in spheres of various sizes**. *Journal of nuclear medicine : official publication, Society of Nuclear Medicine* 1994, **35**(1):152-156.

Siegel JA, Thomas SR, Stubbs JB, Stabin MG, Hays MT, Koral KF, Robertson JS, Howell RW, Wessels BW, Fisher DR *et al*: **MIRD pamphlet no. 16: Techniques for quantitative radiopharmaceutical biodistribution data acquisition and analysis for use in human radiation dose estimates**. *Journal of nuclear medicine : official publication, Society of Nuclear Medicine* 1999, **40**(2):37S-61S.

Slocum JL, Heung M, Pennathur S: **Marking renal injury: can we move beyond serum creatinine?** *Translational research : the journal of laboratory and clinical medicine* 2012, **159**(4):277-289.

RADAR - the RAdiation Dose Assessment Resource

Stabin MG, Siegel JA: **Physical models and dose factors for use in internal dose assessment**. *Health physics* 2003, **85**(3):294-310.

Stabin MG, Siegel JA, Sparks RB, Eckerman KF, Breitz HB: **Contribution to red marrow absorbed dose from total body activity: a correction to the MIRD method**. *Journal of nuclear medicine : official publication, Society of Nuclear Medicine* 2001, **42**(3):492-498.

Stahl AR, Wagner B, Poethko T, Perutka M, Wester HJ, Essler M, Heemann U, Schwaiger M, Lutz J: **Renal accumulation of**

[111In]DOTATOC in rats: influence of inhibitors of the organic ion transport and diuretics. *European journal of nuclear medicine and molecular imaging* 2007, **34**(12):2129-2134.

Stengel A, Rivier J, Tache Y: **Modulation of the adaptive response to stress by brain activation of selective somatostatin receptor subtypes**. *Peptides* 2013, **42**:70-77.

Sward C, Bernhardt P, Ahlman H, Wangberg B, Forssell-Aronsson E, Larsson M, Svensson J, Rossi-Norrlund R, Kolby L: **[177Lu-DOTA 0-Tyr 3]-octreotate treatment in patients with disseminated gastroenteropancreatic neuroendocrine tumors: the value of measuring absorbed dose to the kidney**. *World J Surg* 2010, **34**(6):1368-1372.

Svensson J, Molne J, Forssell-Aronsson E, Konijnenberg M, Bernhardt P: **Nephrotoxicity profiles and threshold dose values for [177Lu]-DOTATATE in nude mice**. *Nuclear medicine and biology* 2012, **39**(6):756-762.

Taal MW, Brenner BM, Rector FC: **Brenner & Rector's the kidney**, 9th edn. Philadelphia, PA: Elsevier/Saunders; 2012.

Terrillon S, Bouvier M: **Roles of G-protein-coupled receptor dimerization**. *EMBO reports* 2004, **5**(1):30-34.

Thomas SR, Maxon HR, Kereiakes JG: **In vivo quantitation of lesion radioactivity using external counting methods**. *Medical physics* 1976, **03**(04):253-255.

Toumpanakis C, Caplin ME: **Update on the role of somatostatin analogs for the treatment of patients with gastroenteropancreatic neuroendocrine tumors**. *Seminars in oncology* 2013, **40**(1):56-68.

Valentin J: **Basic anatomical and physiological data for use in radiological protection: reference values: ICRP Publication 89**. *Annals of the ICRP* 2002, **32**(3):1-277.

Van Binnebeek S, Baete K, Terwinghe C, Vanbilloen B, Haustermans K, Mortelmans L, Borbath I, Van Cutsem E, Verslype C, Mottaghy FM *et al*: **Significant impact of transient deterioration of renal function on dosimetry in PRRT**. *Annals of nuclear medicine* 2013, **27**(1):74-77.

van Essen M, Krenning EP, Kam BL, de Jong M, Valkema R, Kwekkeboom DJ: **Peptide-receptor radionuclide therapy for endocrine tumors**. *Nature reviews Endocrinology* 2009, **5**(7):382-393.

Van Op den Bosch J, Adriaensen D, Van Nassauw L, Timmermans JP: **The role(s) of somatostatin, structurally related peptides and somatostatin receptors in the gastrointestinal tract: a review**. *Regulatory peptides* 2009, **156**(1-3):1-8.

Vegt E, de Jong M, Wetzels JF, Masereeuw R, Melis M, Oyen WJ, Gotthardt M, Boerman OC: **Renal toxicity of radiolabeled peptides and antibody fragments: mechanisms, impact on radionuclide therapy, and strategies for prevention**. *Journal of nuclear*

medicine : official publication, Society of Nuclear Medicine 2010, **51**(7):1049-1058.

Vegt E, Eek A, Oyen WJ, de Jong M, Gotthardt M, Boerman OC: **Albumin-derived peptides efficiently reduce renal uptake of radiolabelled peptides**. *European journal of nuclear medicine and molecular imaging* 2010, **37**(2):226-234.

Wehrmann C, Senftleben S, Zachert C, Muller D, Baum RP: **Results of individual patient dosimetry in peptide receptor radionuclide therapy with 177Lu DOTA-TATE and 177Lu DOTA-NOC**. *Cancer biotherapy & radiopharmaceuticals* 2007, **22**(3):406-416.

Weyer K, Nielsen R, Petersen SV, Christensen EI, Rehling M, Birn H: **Renal uptake of 99mTc-dimercaptosuccinic acid is dependent on normal proximal tubule receptor-mediated endocytosis**. *Journal of nuclear medicine : official publication, Society of Nuclear Medicine* 2013, **54**(1):159-165.

Viguerie N, Esteve JP, Susini C, Vaysse N, Ribet A: **Processing of receptor-bound somatostatin: internalization and degradation by pancreatic acini**. *The American journal of physiology* 1987, **252**(4 Pt 1):G535-542.

Yavropoulou MP, Kotsa K, Pikilidou M, Keisisoglou I, Yovos JG: **Effects of intracerebroventricular infusion of Somatostatin-14 on peripheral glucoregulation in dogs**. *Journal of neuroendocrinology* 2013.